Classical and Bayesian Stress-Strength Reliability Estimation for Weibull Data under Unified Hybrid Censoring Scheme with LED Application

Mazen Nassar[1,2,*], Refah Alotaibi[3] and Ahmed Elshahhat[4]

[1] Department of Statistics, Faculty of Science, King Abdulaziz University, Jeddah, 21589, Saudi Arabia

[2] Department of Statistics, Faculty of Commerce, Zagazig University, Zagazig, 44519, Egypt

[3] Department of Mathematical Sciences, College of Science, Princess Nourah bint Abdulrahman University, P.O. Box 84428, Riyadh, 11671, Saudi Arabia

[4] Faculty of Technology and Development, Zagazig University, Zagazig, 44519, Egypt

INFORMATION

Keywords:
Stress-Strength reliability
unified hybrid
weibull distribution
Bayesian
MCMC
light-emitting diode

DOI: 10.23967/j.rimni.2025.10.69730

SCIPEDIA Revista Internacional de Métodos Numéricos para Cálculo y Diseño en Ingeniería

Revista Internacional Métodos numéricos para cálculo y diseño en ingeniería RIMNI

Classical and Bayesian Stress-Strength Reliability Estimation for Weibull Data under Unified Hybrid Censoring Scheme with LED Application

Mazen Nassar[1,2,*], **Refah Alotaibi**[3] **and Ahmed Elshahhat**[4]

[1]Department of Statistics, Faculty of Science, King Abdulaziz University, Jeddah, 21589, Saudi Arabia

[2]Department of Statistics, Faculty of Commerce, Zagazig University, Zagazig, 44519, Egypt

[3]Department of Mathematical Sciences, College of Science, Princess Nourah bint Abdulrahman University, P.O. Box 84428, Riyadh, 11671, Saudi Arabia

[4]Faculty of Technology and Development, Zagazig University, Zagazig, 44519, Egypt

ABSTRACT

The stress-strength reliability parameter is a key metric used in various fields, including engineering, medicine, and business. In engineering, it quantifies the probability that a system's strength X exceeds the applied stress Y. In this study, we examine for the first time four estimation approaches for evaluating the stress-strength reliability parameter $\mathfrak{R} = P(Y < X)$, where X and Y are independent Weibull random variables with different scale parameters but a common shape parameter. The analysis is conducted under a unified hybrid censoring scheme. From the classical perspective, we employ the maximum likelihood and maximum product of spacings methods to obtain both point and interval estimates. From the Bayesian perspective, two forms of the posterior distribution, based on the likelihood and spacings functions, are derived and analyzed using Markov Chain Monte Carlo sampling techniques. The Bayes estimates of $\mathfrak{R}$ are obtained under the symmetric squared error loss, and the corresponding Bayesian credible intervals are also computed. To compare the four point estimators and the four interval estimators, an extensive simulation study is performed using various experimental scenarios. Finally, comprehensive analyses for organic white light-emitting diode datasets mixed with three colors, namely red, green, and blue, are provided.

OPEN ACCESS

Received: 29/06/2025

Accepted: 16/09/2025

Published: 23/01/2026

DOI
10.23967/j.rimni.2025.10.69730

Keywords:
Stress-Strength reliability
unified hybrid
weibull distribution
Bayesian
MCMC
light-emitting diode

1 Introduction

The stress-strength reliability model is a probability-based measure used to evaluate the performance of a system or component. It estimates the likelihood that a component will fail when the external stress Y it experiences exceeds its internal strength X. The reliability parameter is defined as $\mathfrak{R} = P(Y < X)$, which represents the likelihood of the component surviving under stress. It is important to note that failure occurs if $Y > X$ at any point; otherwise, the component functions as

*Correspondence: Mazen Nassar. (mezo10011@gmail.com)

planned. Since the foundational work of Birnbaum and McCarty [1], the estimation of the reliability parameter $\mathfrak{R}$ and its statistical inferences has been extensively studied in various domains, such as engineering, business, and medical sciences. Kotz et al. [2] presented numerous examples of the stress-strength model. Asgharzadeh et al. [3] noted that the stress-strength reliability model $\mathfrak{R} = P(Y < X)$ is of significant interest beyond traditional reliability analysis. This is because it offers a general way to compare two populations and has applications in various fields. In recent years, many researchers have explored various estimation approaches, including classical and Bayesian methods, for the stress-strength reliability model under the assumptions of different lifetime distributions. Kundu and Gupta [4] analyzed the reliability parameter $\mathfrak{R}$ when X and Y are Weibull (We) random variables sharing the same shape parameter but have distinct scale parameters. Similarly, Pundir and Gupta [5] examined the stress-strength reliability $\mathfrak{R}$ for the Chen distribution using hybrid censoring schemes. See also the work of Jana et al. [6] for exponential distribution, Kumari et al. [7] for Kumaraswamy distribution, and Kotb and Al Omari [8] for exponential-Rayleigh distribution, among others.

The first step in analyzing the stress-strength reliability model is selecting the appropriate statistical distribution to model both variables X and Y. One of the most significant and widely used statistical distributions is the We distribution, which is characterized by one scale parameter and one shape parameter. This distribution is capable of modeling three different failure rates, namely constant, increasing, and decreasing shapes, which commonly appear when modeling engineering and medical data. For more details on the We distribution, its extensions, and applications, refer to Lai et al. [9]. See also the work of Cavalcante et al. [10]. Many authors considered the We distribution when studying the stress-strength reliability model due to its flexibility. Almarashi et al. [11] studied various classical estimation approaches of the stress-strength reliability model for the We distribution. If the random variable X follows the We distribution, then its probability density function (PDF) can be expressed as

$$g(x; \mu, \beta) = \mu\beta x^{\beta-1} e^{-\mu x^{\beta}}, x > 0, \tag{1}$$

where $\mu > 0$ and $\beta > 0$ are the scale and shape parameters, respectively. The corresponding distribution function is given by

$$G(x; \mu, \beta) = 1 - e^{-\mu x^{\beta}}. \tag{2}$$

Let the strength X follows $We(\mu_1, \beta)$ and the stress Y follows $We(\mu_2, \beta)$. Then, under the independent assumption of X and Y, the stress-strength reliability parameter $\mathfrak{R} = P(Y < X)$, can be expressed as

$$\mathfrak{R} = \frac{\mu_1}{\mu_1 + \mu_2}. \tag{3}$$

It is important to note that assuming a common shape parameter is standard in stress–strength reliability studies involving We distributions, as it simplifies the derivation of $\mathfrak{R} = P(Y < X)$ into a closed-form expression, thereby facilitating efficient estimation under the complex UHC scheme. This assumption also reduces computational complexity in classical and Bayesian estimation methods while maintaining model adequacy.

Another important consideration when studying the stress-strength reliability model is whether to work with complete or censored data. In practice, employing complete data is frequently impractical, as experimenters often encounter censored data due to factors such as testing period and associated expenses. Therefore, censored data are naturally used in such investigations. However, the question arises: which censoring plan should be used? The literature suggests a variety of censoring schemes, each with its advantages. Experimenters usually aim to find a plan that balances the test duration with an adequate number of observed failures, thereby allowing efficient statistical inference. The most common classical censoring schemes include Type-I, Type-II, hybrid Type-I, and hybrid Type-II censoring plans, see Balakrishnan and Kundu [12], for more detail. Another two advances in censoring plans are the generalized Type-I and Type-II hybrid censoring (HC) schemes, as proposed by Chandrasekar et al. [13]. Nevertheless, the generalized Type-I HC methodology does not guarantee a predetermined number of failures, while the generalized Type-II HC plan risks observing very few or even no failures. To overpower these disadvantages, Balakrishnan et al. [14] integrated the two censoring methods and presented a unified hybrid censoring (UHC) plan.

Let $X_{1:n}, X_{2:n}, \ldots, X_{n:n}$ denote the ordered failure times in a life testing experiment containing n similar units. Before the experiment starts, the researcher pre-selects two integers r and k, where $1 \leq r < k \leq n$, and two time limits $0 < T_1 < T_2 < \infty$. The UHC plan can be described as follows: (1) If $X_{r:n} < T_1$, end the experiment at $\min\{\max(X_{k:n}, T_1), T_2\}$, (2) If $T_1 < X_{r:n} < T_2$, terminate the experiment at $\min(X_{k:n}, T_2)$, and (3) If $X_{r:n} > T_2$, conclude the test at $X_{r:n}$. Accordingly, employing the UHC plan lead to one of the following six cases

- Case 1: If $0 < X_{r:n} < X_{k:n} < T_1 < T_2$, set $\tau = T_1$.
- Case 2: If $0 < X_{r:n} < T_1 < X_{k:n} < T_2$, set $\tau = X_{k:n}$.
- Case 3: If $0 < X_{r:n} < T_1 < T_2 < X_{k:n}$, set $\tau = T_2$.
- Case 4: If $0 < T_1 < X_{r:n} < X_{k:n} < T_2$, set $\tau = X_{k:n}$.
- Case 5: If $0 < T_1 < X_{r:n} < T_2 < X_{k:n}$, set $\tau = T_2$.
- Case 6: If $0 < T_1 < T_2 < X_{r:n} < X_{k:n}$, set $\tau = X_{r:n}$,

where τ refers to the time point at which the test is terminated. Let d refers to the observed number of failures defined as

$$d = \begin{cases} a, & \text{for Case 1,} \\ k, & \text{for Cases 2 and 4,} \\ b, & \text{for Cases 3 and 5,} \\ r, & \text{for Case 6,} \end{cases}$$

where a and b denote the number of observed failures occurred before T_1 and T_2, respectively. Fig. 1 shows the various possible cases of UHC plan.

Let $\underline{\mathbf{x}} = (x_1, \ldots, x_d)$ represent an observed UHC sample, where $x_i = x_{i:n}$ for simplicity. Then, the joint likelihood function (LF) can be expressed, omitting the constant term, as:

$$L(\boldsymbol{\theta}; \underline{\mathbf{x}}) = \prod_{i=1}^{d} f(x_i) \left[1 - F(\tau)\right]^{n-d}, \tag{4}$$

where $\boldsymbol{\theta}$ is the vector of the unknown parameters. Many studies considered the UHC plan using various lifetime distributions, and some recent works include Hasaballah et al. [15] for generalized inverted exponential distribution, Kumar et al. [16] for inverse Pareto distribution, Hasaballah et al. [17] for power rayleigh distribution, and Shukla et al. [18] for power Lindley distribution. By maximizing the logarithm of the LF in (4) with respect to $\boldsymbol{\theta}$, the maximum likelihood estimators (MLEs) can be obtained. Another classical estimation approach, known as the maximum product of spacings (MPS) method, was proposed independently by Cheng and Amin [19] and Ranneby [20] as a competitive alternative to the maximum likelihood method. As noted by Anatolyev and Kosenok [21], it has been observed that the MPS estimators (MPSEs) are more efficient than the MLEs for skewed distributions or in small sample cases. Based on an observed UHC sample $\underline{\mathbf{x}}$, the MPSEs are obtained by maximizing the following product of spacings function (SF)

$$P(\boldsymbol{\theta}; \underline{\mathbf{x}}) = \prod_{i=1}^{d+1} [F(x_i) - F(x_{i-1})] [1 - F(\tau)]^{n-d}. \tag{5}$$

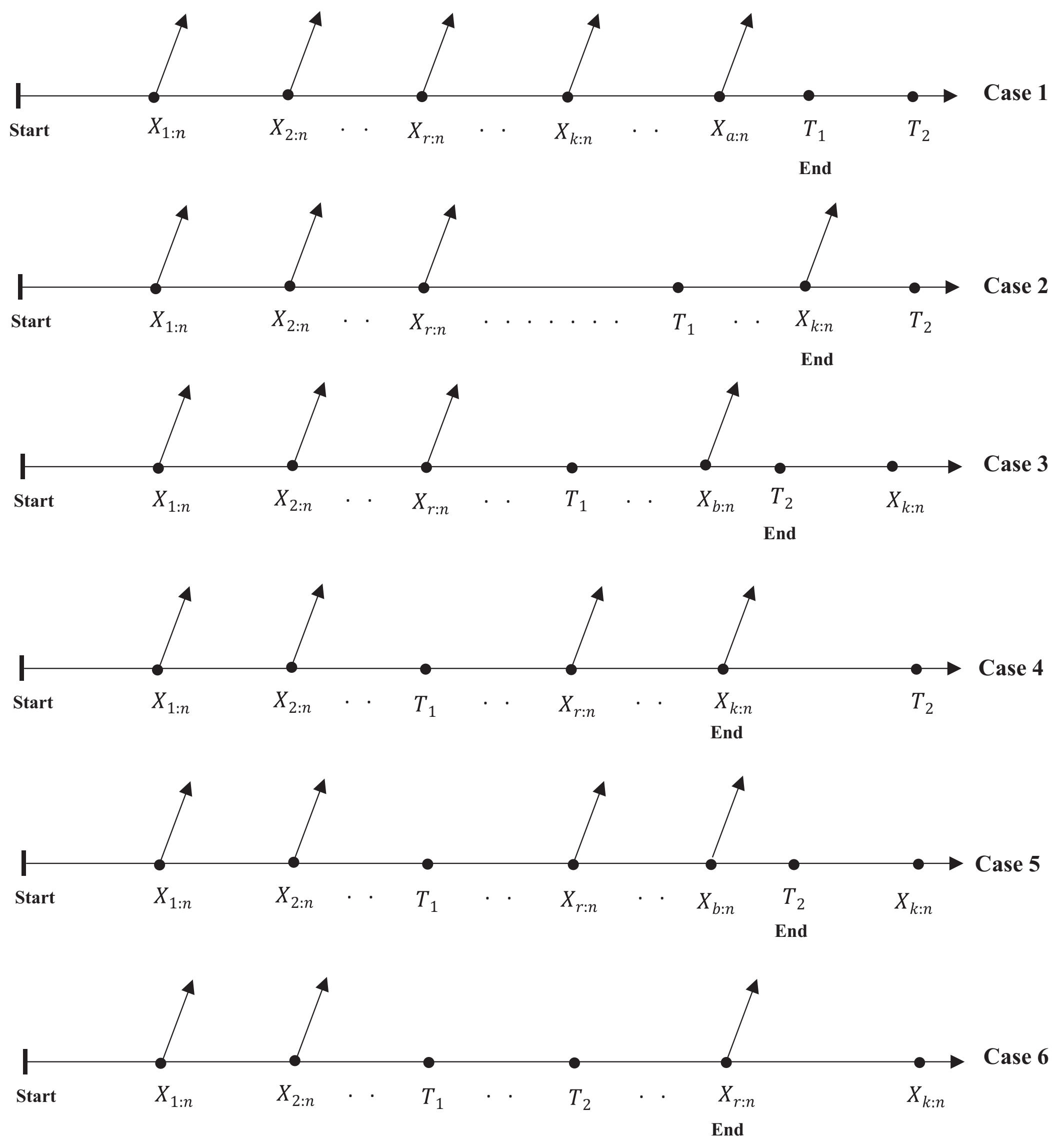

Figure 1: Schematic representation of UHC plan

It is important to mention that after obtaining the MLEs of the model parameters, the MLE of the stress-strength reliability parameter $\mathfrak{R} = P(Y < X)$ can be easily derived by applying the invariance property of the MLEs, as well as the MPSEs, as will be discussed in the following sections.

This study aims to investigate both classical and Bayesian estimations of the stress-strength reliability parameter of the We distribution using UHC plan. We compare four estimation approaches: (1) Maximum likelihood estimation, which is standard but can be inefficient with heavy censoring, (2) MPS estimation, introduced here for the first time under UHC scheme, (3) Bayesian estimation based on the LF, incorporating prior information via traditional posteriors, and (4) Bayesian estimation based on the SF, yielding an alternative posterior form that aligns with order statistic properties in censored data. Prior studies on stress-strength reliability have primarily relied on the maximum likelihood estimation method or basic Bayesian methods via LF, see for example Hu and Ren [22], and Kotb and Raqab [23]. However, these approaches overlook the potential of MPS, which has shown superiority in spacings-based inference for censored samples, see Kateri and Nikolov [24]. Our work fills these gaps by: (1) Deriving MPSEs using UHC scheme which often yielding better estimates in small samples or with censoring, (2) Developing two Bayesian posteriors (LF- and SF-based) and using Markov Chain Monte Carlo (MCMC) under squared error loss for point estimates and credible intervals, enhancing uncertainty quantification, and (3) Comparing the four estimation methods which has not been done previously in this unified framework.

It is worth noting that this is the first time the MPS estimation method has been considered under the UHC scheme. This work is motivated by the following factors: (1) The widespread use of the We distribution for modeling various types of data across many fields, (2) The significance of the UHC scheme, which ensures that the experiment is completed within a maximum time T_2 with at least r failures. If this condition is not met, the scheme guarantees exactly r failures, and (3) The broad applicability of the stress-strength reliability model in diverse fields, particularly in reliability engineering. We believe that comparing various estimation methods for the stress-strength reliability parameter of the We distribution will be of great interest to many readers, particularly reliability engineers and practicing statisticians. The comparison of the four estimation methods discussed is driven by the practical challenges in reliability engineering, where censored data under UHC are common due to time-constrained experiments. Each method offers distinct advantages. By comparing these methods, we aim to provide reliability engineers with evidence-based guidance on selecting the most effective estimator for the stress-strength reliability metric using UHC scenarios, where no prior study has systematically evaluated all four approaches together. While classical and Bayesian approaches differ in their inferential frameworks, their comparison is both appropriate and valuable in the context of stress-strength reliability estimation. All methods target the same parameter, $\mathfrak{R} = P(Y < X)$, and are evaluated using comparable performance metrics, as detailed in the simulation study presented later. To achieve our objective, we first derive both classical point and interval estimates for the stress-strength reliability parameter. The interval estimates are computed using the asymptotic properties of both MLEs and MPSEs. Next, we incorporate Bayesian estimations using the squared error loss function and the MCMC procedure. In our analysis, we consider two different forms of the posterior distribution obtained using the LF and the SF. Additionally, Bayes credible intervals (BCIs) for the reliability parameter are derived. We then conduct a relative comparison of the classical and Bayesian estimation methods through simulations. Finally, we demonstrate the practicality of our approach using light-emitting diode (LED) data.

The remainder of this paper is organized as follows. In Section 2, we discuss the MLE of $\mathfrak{R}$ and the associated approximate confidence interval (ACI). Section 3 derives the MPSE along with the ACI. In Section 4, we detail the Bayesian estimation approaches using the LF and the SF. The simulation design and numerical results are presented in Section 5. Section 6 provides the results of LED application. Finally, we conclude the paper in Section 7.

2 Likelihood Estimation

Let $\underline{\mathbf{x}}$ represent an observed UHC sample of size d drawn from n units, where $X \sim We(\mu_1, \beta)$. Let $\underline{\mathbf{y}}$ represent an observed UHC sample of size q out of m items, where $Y \sim We(\mu_2, \beta)$. The UHC sample $\underline{\mathrm{y}}$ is selected using the two predetermined integers r^* and k^*, where $1 \leq r^* < k^* \leq m$, and two time limits $0 < T_1^* < T_2^* < \infty$ using the same methodology discussed in the previous section. Let $\boldsymbol{\theta} = (\mu_1, \mu_2, \beta)^\top$, then the joint LF of $\boldsymbol{\theta}$ can be expressed as follows

$$L(\boldsymbol{\theta}; \underline{\mathbf{x}}, \underline{\mathbf{y}}) = \left\{ \prod_{i=1}^{d} f(x_i) \left[1 - F(\tau)\right]^{n-d} \right\} \left\{ \prod_{i=1}^{q} f(y_i) \left[1 - F(\eta)\right]^{m-q} \right\}, \tag{6}$$

where

$$(q, \eta) = \begin{cases} (a^*, T_1^*), & \text{for Case 1}, \\ (k^*, y_{k^*}), & \text{for Cases 2 and 4}, \\ (b^*, T_2^*), & \text{for Cases 3 and 5}, \\ (r^*, y_{r^*}), & \text{for Case 6}, \end{cases}$$

where a^* and b^* refer to the observed number of failures recorded before T_1^* and T_2^*, respectively. Based on (1), (2) and (6), the joint LF follows

$$L(\boldsymbol{\theta}; \underline{\mathbf{x}}, \underline{\mathbf{y}}) = \mu_1^d \mu_2^q \beta^{d+q} \exp\left\{ (\beta - 1) Q - \mu_1 \varphi(\underline{\mathbf{x}}; \beta) - \mu_2 \psi(\underline{\mathbf{y}}; \beta) \right\}, \tag{7}$$

where $Q = \sum_{i=1}^{d} \log(x_i) + \sum_{i=1}^{q} \log(y_i)$, $\varphi(\underline{\mathbf{x}}; \beta) = \sum_{i=1}^{d} x_i^\beta + (n-d)\tau^\beta$, and $\psi(\underline{\mathbf{y}}; \beta) = \sum_{i=1}^{q} y_i^\beta + (m-q)\eta^\beta$. The log-LF can be expressed as

$$\mathcal{L}(\boldsymbol{\theta}; \underline{\mathbf{x}}, \underline{\mathbf{y}}) = d \log(\mu_1) + q \log(\mu_2) + (d+q) \log(\beta) + (\beta - 1) Q - \mu_1 \varphi(\underline{\mathbf{x}}; \beta) - \mu_2 \psi(\underline{\mathbf{y}}; \beta). \tag{8}$$

The MLEs of μ_1, μ_2 and β, denoted by $\hat{\mu}_1, \hat{\mu}_2$ and $\hat{\beta}$, can be acquired by solving the following likelihood equations

$$\frac{\partial \mathcal{L}(\boldsymbol{\theta}; \underline{\mathbf{x}}, \underline{\mathbf{y}})}{\partial \mu_1} = \frac{d}{\mu_1} - \varphi(\underline{\mathbf{x}}; \beta) = 0, \quad \frac{\partial \mathcal{L}(\boldsymbol{\theta}; \underline{\mathbf{x}}, \underline{\mathbf{y}})}{\partial \mu_2} = \frac{q}{\mu_2} - \psi(\underline{\mathbf{y}}; \beta) = 0 \tag{9}$$

and

$$\frac{\partial \mathcal{L}(\boldsymbol{\theta}; \underline{\mathbf{x}}, \underline{\mathbf{y}})}{\partial \beta} = \frac{d+q}{\beta} + Q - \mu_1 \varphi_1(\underline{\mathbf{x}}; \beta) - \mu_2 \psi_1(\underline{\mathbf{y}}; \beta) = 0, \tag{10}$$

where $\varphi_1(\underline{\mathbf{x}}; \beta) = \sum_{i=1}^{d} x_i^\beta \log(x_i) + (n-d)\tau^\beta \log(\tau)$, and $\psi_1(\underline{\mathbf{y}}; \beta) = \sum_{i=1}^{q} y_i^\beta \log(y_i) + (m-q)\eta^\beta \log(\eta)$. From (9), we can derive the MLEs $\hat{\mu}_1$ and $\hat{\mu}_2$

$$\hat{\mu}_1(\beta) = \frac{d}{\varphi(\underline{\mathbf{x}}; \beta)}, \quad \text{and} \quad \hat{\mu}_2(\beta) = \frac{q}{\psi(\underline{\mathbf{y}}; \beta)}. \tag{11}$$

By substituting the expressions for $\hat{\mu}_1(\beta)$ and $\hat{\mu}_2(\beta)$ into (10), the MLE $\hat{\beta}$ can be acquired as the solution of $\zeta(\beta) = \beta$, with

$$\zeta(\beta) = \left[\frac{d\varphi_1(\underline{\mathbf{x}}; \beta)/\varphi(\underline{\mathbf{x}}; \beta) + q\psi_1(\underline{\mathbf{y}}; \beta)/\psi(\underline{\mathbf{y}}; \beta) - Q}{d+q} \right]^{-1}. \tag{12}$$

Employing the iterative procedure, defined as $\zeta(\beta^{(j)}) = \beta^{(j+1)}$, where $\beta^{(j)}$ represents the j-th iteration, the Eq. (12) can be solved. Once $\hat{\beta}$ is computed, the MLEs of μ_1 and μ_2 can be derived from (11) as $\hat{\mu}_1 = \hat{\mu}_1(\hat{\beta})$ and $\hat{\mu}_2 = \hat{\mu}_2(\hat{\beta})$. After obtaining the MLEs $\hat{\mu}_1, \hat{\mu}_2$ and $\hat{\beta}$, we can utilize the invariance property of the MLEs to compute the MLE of the stress-strength reliability parameter $\mathfrak{R}$ using (3) as follows

$$\hat{\mathfrak{R}} = \frac{d\psi(\underline{\mathbf{y}};\hat{\beta})}{d\psi(\underline{\mathbf{y}};\hat{\beta}) + q\varphi(\underline{\mathbf{x}};\hat{\beta})}.$$

Sayyareh and Panahi [25] studied the asymptotic distribution of the MLEs under UHC scheme and proved that the asymptotic distribution of the MLEs is asymptotically normal. We employ this result as well as the delta method in order to develop the ACI of the stress-strength reliability measure. To construct the ACI for $\mathfrak{R}$, it is essential to derive the variance associated with its MLE. According to Asgharzadeh et al. [3], the requisite variance can be determined using the delta method. This approach necessitates the computation of the variance-covariance matrix of the unknown parameters. Given the complexity involved in obtaining the Fisher information matrix, we estimate the variance-covariance matrix by inverting the observed Fisher information matrix as follows

$$\mathbf{\Sigma}(\hat{\boldsymbol{\theta}}) = \begin{bmatrix} -F_{11} & 0 & -F_{13} \\ & -F_{22} & -F_{23} \\ & & -F_{33} \end{bmatrix}^{-1} = \begin{bmatrix} \hat{\Sigma}_{11} & 0 & \hat{\Sigma}_{13} \\ & \hat{\Sigma}_{22} & \hat{\Sigma}_{23} \\ & & \hat{\Sigma}_{33} \end{bmatrix}, \tag{13}$$

where $F_{ij}, i,j = 1,2,3$, are evaluated at $\hat{\boldsymbol{\theta}} = (\hat{\mu}_1, \hat{\mu}_2, \hat{\beta})^\top$, and given by

$$F_{11} = -\frac{d}{\mu_1^2}, \quad F_{22} = -\frac{q}{\mu_2^2},$$
$$F_{33} = -\frac{d+q}{\beta^2} - \mu_1\varphi_2(\underline{\mathbf{x}};\beta) - \mu_2\psi_2(\underline{\mathbf{y}};\beta),$$
$$F_{13} = -\varphi_1(\underline{\mathbf{x}};\beta), \quad \text{and} \quad F_{23} = -\psi_1(\underline{\mathbf{y}};\beta),$$

where $\varphi_2(\underline{\mathbf{x}};\beta) = \sum_{i=1}^{d} x_i^\beta \log^2(x_i) + (n-d)\tau^\beta \log^2(\tau)$, and $\psi_2(\underline{\mathbf{y}};\beta) = \sum_{i=1}^{q} y_i^\beta \log^2(y_i) + (m-q)\eta^\beta \log^2(\eta)$. Using the delta method, we can approximate the variance of $\hat{\mathfrak{R}}$ as follows

$$\hat{\Sigma}_{\mathfrak{R}} \simeq \frac{1}{(\hat{\mu}_1+\hat{\mu}_2)^2}[\hat{\mu}_2, -\hat{\mu}_1, 0] \begin{bmatrix} \hat{\Sigma}_{11} & 0 & \hat{\Sigma}_{13} \\ & \hat{\Sigma}_{22} & \hat{\Sigma}_{23} \\ & & \hat{\Sigma}_{33} \end{bmatrix} \begin{bmatrix} \hat{\mu}_2 \\ -\hat{\mu}_1 \\ 0 \end{bmatrix}$$
$$\simeq \frac{\hat{\mu}_2^2\hat{\Sigma}_{11} + \hat{\mu}_1^2\hat{\Sigma}_{22}}{(\hat{\mu}_1+\hat{\mu}_2)^2},$$

Accordingly, the $100\%(1-\alpha)$ ACI of the stress-strength reliability parameter $\mathfrak{R}$ can be computed as

$$\left(\frac{\hat{\mu}_1 - z_{\alpha/2}\sqrt{\hat{\mu}_2^2\hat{\Sigma}_{11} + \hat{\mu}_1^2\hat{\Sigma}_{22}}}{\hat{\mu}_1+\hat{\mu}_2}, \frac{\hat{\mu}_1 + z_{\alpha/2}\sqrt{\hat{\mu}_2^2\hat{\Sigma}_{11} + \hat{\mu}_1^2\hat{\Sigma}_{22}}}{\hat{\mu}_1+\hat{\mu}_2}\right),$$

where $z_{\alpha/2}$ is the upper $(\alpha/2)^{th}$ percentile point of $N(0,1)$.

3 Product of Spacings Estimation

In this section, the MSPE and ACI of the stress-strength reliability parameter of the We distribution is derived based on the UHC data. Based on the two UHC samples, denoted by $\underline{\mathbf{x}}$ and $\underline{\mathbf{y}}$, where $X \sim We(\mu_1, \beta)$ and $Y \sim We(\mu_2, \beta)$, we can write the SF of $\boldsymbol{\theta}$ in (5) as follows

$$P(\boldsymbol{\theta}; \underline{\mathbf{x}}, \underline{\mathbf{y}}) = \left\{ \prod_{i=1}^{d+1} [F(x_i) - F(x_{i-1})] [1 - F(\tau)]^{n-d} \right\} \left\{ \prod_{i=1}^{q+1} [F(y_i) - F(y_{i-1})] [1 - F(\eta)]^{m-q} \right\}. \tag{14}$$

Using (1), (2) and (14), the joint SF can be expressed as

$$P(\boldsymbol{\theta}; \underline{\mathbf{x}}, \underline{\mathbf{y}}) = \exp \left\{ \sum_{i=1}^{d+1} \omega(x_i; \mu_1, \beta) - \mu_1 \varphi(\underline{\mathbf{x}}; \beta) + \sum_{i=1}^{q+1} \nu(y_i; \mu_2, \beta) - \mu_2 \psi(\underline{\mathbf{y}}; \beta) \right\}, \tag{15}$$

where $\omega(x_i; \mu_1, \beta) = \log \left[e^{\mu_1 (x_i^{\beta} - x_{i-1}^{\beta})} - 1 \right]$ and $\nu(y_i; \mu_2, \beta) = \log \left[e^{\mu_2 (y_i^{\beta} - y_{i-1}^{\beta})} - 1 \right]$. The log-SF can be obtained using (15) as

$$\mathcal{P}(\boldsymbol{\theta}; \underline{\mathbf{x}}, \underline{\mathbf{y}}) = \sum_{i=1}^{d+1} \omega(x_i; \mu_1, \beta) - \mu_1 \varphi(\underline{\mathbf{x}}; \beta) + \sum_{i=1}^{q+1} \nu(y_i; \mu_2, \beta) - \mu_2 \psi(\underline{\mathbf{y}}; \beta). \tag{16}$$

The MPSEs of the unknown parameters μ_1, μ_2 and β, denoted by $\tilde{\mu}_1, \tilde{\mu}_2$ and $\tilde{\beta}$, can be obtained by maximizing the objective function in (15) with respect to these three parameters. Alternatively, they can be obtained by solving the following three normal equations.

$$\frac{\partial \mathcal{P}(\boldsymbol{\theta}; \underline{\mathbf{x}}, \underline{\mathbf{y}})}{\partial \mu_1} = \sum_{i=1}^{d+1} \omega_1(x_i; \mu_1, \beta) - \varphi(\underline{\mathbf{x}}; \beta) = 0, \tag{17}$$

$$\frac{\partial \mathcal{P}(\boldsymbol{\theta}; \underline{\mathbf{x}}, \underline{\mathbf{y}})}{\partial \mu_2} = \sum_{i=1}^{q+1} \nu_1(y_i; \mu_2, \beta) - \psi(\underline{\mathbf{y}}; \beta) = 0, \tag{18}$$

and

$$\frac{\partial \mathcal{P}(\boldsymbol{\theta}; \underline{\mathbf{x}}, \underline{\mathbf{y}})}{\partial \beta} = \sum_{i=1}^{d+1} \omega_2(x_i; \mu_1, \beta) - \mu_1 \varphi_1(\underline{\mathbf{x}}; \beta) + \sum_{i=1}^{q+1} \nu_2(y_i; \mu_2, \beta) - \mu_2 \psi_1(\underline{\mathbf{y}}; \beta) = 0, \tag{19}$$

where

$$\omega_1(x_i; \mu_1, \beta) = \frac{x_i^{\beta} - x_{i-1}^{\beta}}{1 - e^{-\mu_1 (x_i^{\beta} - x_{i-1}^{\beta})}}, \quad \omega_2(x_i; \mu_1, \beta) = \frac{\mu_1 [x_i^{\beta} \log(x_i) - x_{i-1}^{\beta} \log(x_{i-1})]}{1 - e^{-\mu_1 (x_i^{\beta} - x_{i-1}^{\beta})}},$$

and

$$\nu_1(y_i; \mu_2, \beta) = \frac{y_i^{\beta} - y_{i-1}^{\beta}}{1 - e^{-\mu_2 (y_i^{\beta} - y_{i-1}^{\beta})}}, \quad \nu_2(y_i; \mu_2, \beta) = \frac{\mu_2 [y_i^{\beta} \log(y_i) - y_{i-1}^{\beta} \log(y_{i-1})]}{1 - e^{-\mu_2 (y_i^{\beta} - y_{i-1}^{\beta})}}.$$

The normal equations provided by (17)–(19) do not have explicit closed-form solutions. To solve them numerically, iterative techniques such as the Newton-Raphson method can be employed. Once the MPSEs are determined, the MPSE of the stress-strength reliability parameter can be calculated using the invariance property of MPSEs as

$$\tilde{\mathfrak{R}} = \frac{\tilde{\mu}_1}{\tilde{\mu}_1 + \tilde{\mu}_2}.$$

Similar to the process of deriving the ACI for the stress-strength reliability parameter using MLEs, we can also construct the ACI for the reliability parameter $\mathfrak{R}$ utilizing the asymptotic properties of the MPSEs. To establish this ACI, it is critical to first estimate the variance-covariance matrix by inverting the observed Fisher information matrix. The elements of the observed Fisher information matrix in this context are derived from the log-SF presented in Eq. (16). Consequently, we can obtain the estimated variance-covariance matrix as

$$\boldsymbol{\Sigma}^*(\tilde{\boldsymbol{\theta}}) = \begin{bmatrix} -F_{11}^* & 0 & -F_{13}^* \\ & -F_{22}^* & -F_{23}^* \\ & & -F_{33}^* \end{bmatrix}^{-1} = \begin{bmatrix} \tilde{\Sigma}_{11}^* & 0 & \tilde{\Sigma}_{13}^* \\ & \tilde{\Sigma}_{22}^* & \tilde{\Sigma}_{23}^* \\ & & \tilde{\Sigma}_{33}^* \end{bmatrix}, \tag{20}$$

with the fact that the elements $F_{ij}^*, i, j = 1, 2, 3$, are obtained at $\tilde{\boldsymbol{\theta}} = (\tilde{\mu}_1, \tilde{\mu}_2, \tilde{\beta})^\top$, and

$$F_{11}^* = \sum_{i=1}^{d+1} \omega_{11}(x_i; \mu_1, \beta), \quad F_{22}^* = \sum_{i=1}^{q+1} \nu_{11}(y_i; \mu_2, \beta),$$

$$F_{33}^* = \sum_{i=1}^{d+1} \omega_{22}(x_i; \mu_1, \beta) - \mu_1 \varphi_2(\underline{\mathbf{x}}; \beta) + \sum_{i=1}^{q+1} \nu_{22}(y_i; \mu_2, \beta) - \mu_2 \psi_2(\underline{\mathbf{y}}; \beta),$$

$$F_{13}^* = \sum_{i=1}^{d+1} \omega_{13}(x_i; \mu_1, \beta) - \varphi_1(\underline{\mathbf{x}}; \beta), \quad \text{and} \quad F_{23}^* = \sum_{i=1}^{d+1} \nu_{13}(y_i; \mu_2, \beta) - \psi_1(\underline{\mathbf{x}}; \beta),$$

where

$$\omega_{11}(x_i; \mu_1, \beta) = -\omega_1^2(x_i; \mu_1, \beta) e^{-\mu_1 (x_i^\beta - x_{i-1}^\beta)}, \quad \nu_{11}(y_i; \mu_2, \beta) = -\nu_1^2(y_i; \mu_2, \beta) e^{-\mu_2 (y_i^\beta - y_{i-1}^\beta)},$$

$$\omega_{22}(x_i; \mu_1, \beta) = \frac{\omega_1(x_i; \mu_1, \beta)[x_i^\beta \log^2(x_i) - x_{i-1}^\beta \log^2(x_{i-1})]}{[x_i^\beta \log(x_i) - x_{i-1}^\beta \log(x_{i-1})]} - \omega_1^2(x_i; \mu_1, \beta) e^{-\mu_1 (x_i^\beta - x_{i-1}^\beta)},$$

$$\nu_{22}(y_i; \mu_2, \beta) = \frac{\nu_1(y_i; \mu_2, \beta)[y_i^\beta \log^2(y_i) - y_{i-1}^\beta \log^2(y_{i-1})]}{[y_i^\beta \log(y_i) - y_{i-1}^\beta \log(y_{i-1})]} - \nu_1^2(y_i; \mu_2, \beta) e^{-\mu_2 (y_i^\beta - y_{i-1}^\beta)},$$

$$\omega_{13}(x_i; \mu_1, \beta) = \frac{\omega_2(x_i; \mu_1, \beta)}{\mu_1} \left[1 - \mu_1 \omega_1(x_i; \mu_1, \beta) e^{-\mu_1 (x_i^\beta - x_{i-1}^\beta)}\right],$$

and

$$\nu_{13}(y_i; \mu_2, \beta) = \frac{\nu_2(y_i; \mu_2, \beta)}{\mu_2} \left[1 - \mu_2 \nu_1(y_i; \mu_2, \beta) e^{-\mu_2 (y_i^\beta - y_{i-1}^\beta)}\right].$$

Then, after applying the delta method as discussed in the previous section to approximate the variance of the stress-strength reliability parameter using the MPSEs of the model parameter and the estimated variance-covariance matrix in (20), we can compute the $100\%(1-\alpha)$ ACI of $\mathfrak{R}$ as

$$\left(\frac{\tilde{\mu}_1 - z_{\alpha/2}\sqrt{\tilde{\mu}_2^2\tilde{\Sigma}_{11}^* + \tilde{\mu}_1^2\tilde{\Sigma}_{22}^*}}{\tilde{\mu}_1 + \tilde{\mu}_2}, \frac{\tilde{\mu}_1 + z_{\alpha/2}\sqrt{\tilde{\mu}_2^2\tilde{\Sigma}_{11}^* + \tilde{\mu}_1^2\tilde{\Sigma}_{22}^*}}{\tilde{\mu}_1 + \tilde{\mu}_2}\right).$$

4 Bayesian Estimation

Utilizing the assumption that the three parameters μ_1, μ_2, and β are independent random variables, this section examines the Bayesian analysis of the stress-strength reliability parameter $\mathfrak{R}$. In the context of large sample sizes or fully observed data, classical estimation methods generally yield precise results. Conversely, in the case of small sample sizes or censored data, these methods may produce misleading outcomes. In contrast, the Bayesian approach integrates prior information, facilitating more accurate estimations. Additional background on data modeling and Bayesian analysis can be found in Wang et al. [26,27]. The initial step involves identifying the appropriate prior distribution for each parameter. It is important to note that the gamma distribution serves as a conjugate prior for scale and rate parameters in exponential family models, enabling tractable posterior updates and improving computational efficiency. Second, the gamma distribution is highly flexible: depending on its hyperparameters, it can encode both informative and weakly informative priors. Third, in the context of censored data and survival analysis, the gamma prior is particularly useful because its parameters have clear interpretations in terms of prior expected failure rates; for additional details, see Dey et al. [28]. Analyzing the LF, which exhibits a simpler form compared to the SF, reveals that the natural conjugate priors for the parameters μ_1 and μ_2 are gamma distributions. Conversely, no conjugate prior exists for the parameter β. In this context, we also consider employing a gamma prior for this parameter, owing to the flexible characteristics of the gamma distribution, which offers the same support for β.

Suppose that $\mu_1 \sim Gamma(\epsilon_1, \varepsilon_1)$, $\mu_2 \sim Gamma(\epsilon_2, \varepsilon_2)$, and $\beta \sim Gamma(\epsilon_3, \varepsilon_3)$, where $\epsilon_j, \varepsilon_j > 0, j = 1, 2, 3$ are known hyper-parameters. Then, we can formulate the joint prior distribution of $\boldsymbol{\theta}$ as

$$\pi(\boldsymbol{\theta}) \propto \mu_1^{\epsilon_1 - 1}\mu_2^{\epsilon_2 - 1}\beta^{\epsilon_3 - 1}\exp\{\varepsilon_1\mu_1 - \varepsilon_2\mu_2 - \varepsilon_3\beta\}, \ \mu_1, \mu_2, \beta > 0. \tag{21}$$

The posterior distribution of the unknown parameters is obtained by combining the observed data with the prior distribution through Bayes' theorem. In this study, we consider two sources of observed data, resulting in two forms of the posterior distribution. The first is based on the LF, while the second is derived using the SF, for more details, see Kurdi et al. [29]. Based on the LF in (7) and the joint prior distribution in (21), the posterior distribution derived using the LF-based approach can be expressed as

$$W_1(\boldsymbol{\theta}|\underline{\mathbf{x}}, \underline{\mathbf{y}}) = \frac{1}{A_1}\mu_1^{d+\epsilon_1 - 1}\mu_2^{q+\epsilon_2 - 1}\beta^{d+q+\epsilon_3 - 1}\exp\left\{\beta(Q - \varepsilon_3) - \mu_1[\varphi(\underline{\mathbf{x}};\beta) + \varepsilon_1] - \mu_2[\psi(\underline{\mathbf{y}};\beta) + \varepsilon_2]\right\}, \tag{22}$$

where

$$A_1 = \int_0^\infty\int_0^\infty\int_0^\infty \pi(\boldsymbol{\theta})L(\boldsymbol{\theta};\underline{\mathbf{x}}, \underline{\mathbf{y}})d\mu_1 d\mu_2 d\beta.$$

On the other hand, we can obtain the posterior distribution based on the SF-based approach by combining the SF given by (15) with the joint prior distribution provided by (21), as follows

$$W_2(\boldsymbol{\theta}|\underline{\mathbf{x}},\underline{\mathbf{y}}) = \frac{1}{A_2}\mu_1^{\epsilon_1-1}\mu_2^{\epsilon_2-1}\beta^{\epsilon_3-1}\exp\left\{\sum_{i=1}^{d+1}\omega(x_i;\mu_1,\beta) - \mu_1[\varphi(\underline{\mathbf{x}};\beta)+\varepsilon_1]\right.$$
$$\left. + \sum_{i=1}^{q+1}\nu(y_i;\mu_2,\beta) - \mu_2[\psi(\underline{\mathbf{y}};\beta)+\varepsilon_2] - \varepsilon_3\beta\right\}, \tag{23}$$

where

$$A_2 = \int_0^\infty\int_0^\infty\int_0^\infty \pi(\boldsymbol{\theta})P(\boldsymbol{\theta};\underline{\mathbf{x}},\underline{\mathbf{y}})d\mu_1 d\mu_2 d\beta.$$

Under the squared error loss function, the Bayes estimator of the stress-strength reliability parameter $\mathfrak{R}$ is given by the posterior mean. However, both forms of the posterior distribution lack closed-form expressions, making analytical computation of the Bayes estimators infeasible. To overcome this limitation, numerical approximation techniques such as the MCMC procedures can be employed. These methods generate samples from the posterior distribution to approximate the value of $\mathfrak{R}$. To implement the MCMC procedures, we begin with the posterior distribution obtained through the LF-based approach. The initial step in this process involves deriving the full conditional distributions, which will serve as the basis for generating samples. From the target distribution presented in (22), we have the following

$$\mu_1|\boldsymbol{\theta}_{-\mu_1},\underline{\mathbf{x}},\underline{\mathbf{y}} \sim Gamma\left(d+\epsilon_1, \varphi(\underline{\mathbf{x}};\beta)+\varepsilon_1\right), \tag{24}$$

$$\mu_2|\boldsymbol{\theta}_{-\mu_2},\underline{\mathbf{x}},\underline{\mathbf{y}} \sim Gamma\left(q+\epsilon_2, \psi(\underline{\mathbf{y}};\beta)+\varepsilon_2\right), \tag{25}$$

and

$$W_1(\beta|\boldsymbol{\theta}_{-\beta},\underline{\mathbf{x}},\underline{\mathbf{y}}) \propto \beta^{d+q+\epsilon_3-1}\exp\left\{\beta(Q-\varepsilon_3) - \mu_1\varphi(\underline{\mathbf{x}};\beta) - \mu_2\psi(\underline{\mathbf{y}};\beta)\right\}. \tag{26}$$

It is evident from (24) and (25) that generating samples for μ_1 and μ_2 can be straightforwardly implemented. However, it is worth noting that the full conditional distribution of β, given by (26), does not correspond to any well-known statistical distribution. Consequently, we employ the Metropolis-Hastings (M-H) algorithm with a normal proposal distribution within the Gibbs sampler to generate the required MCMC samples for obtaining Bayesian point and interval estimates. To implement the proposed hybrid algorithm, we follow the next steps (Algorithm 1):

Algorithm 1: MCMC sample generation using LF

Step 1. Set $j=1$ and the starting values $\left(\mu_1^{(0)},\mu_2^{(0)},\beta^{(0)}\right)$. Use the MLEs as starting values.
Step 2. Obtain $\beta^{(j)}$ from (26) via the M-H algorithm:
- Generate β^* from $N\left(\beta^{(j-1)},\hat{\Sigma}_{33}\right)$.
- Compute the acceptance ratio:

$$\varrho = \min\left[1, \frac{W_1(\beta^*|\mu_1^{(j-1)},\mu_2^{(j-1)},\underline{\mathbf{x}},\underline{\mathbf{y}})}{W_1(\beta^{(j-1)}|\mu_1^{(j-1)},\mu_2^{(j-1)},\underline{\mathbf{x}},\underline{\mathbf{y}})}\right].$$

(Continued)

Algorithm 1 (continued)

- Draw u from the unit uniform distribution.
- If $u \leq \varrho$, set $\beta^{(j)} = \beta^{*}$. Otherwise, set $\beta^{(j)} = \beta^{(j-1)}$.

Step 3. Generate $\mu_1^{(j)}$ using $Gamma\left(d + \epsilon_1, \varphi(\underline{\mathbf{x}}; \beta^{(j)}) + \varepsilon_1\right)$.

Step 4. Simulate $\mu_2^{(j)}$ from $Gamma\left(q + \epsilon_2, \psi(\underline{\mathbf{y}}; \beta^{(j)}) + \varepsilon_2\right)$.

Step 5. Compute the stress-strength reliability parameter at iteration j as:

$$\mathfrak{R}^{(j)} = \frac{\mu_1^{(j)}}{\mu_1^{(j)} + \mu_2^{(j)}}.$$

Step 6. Update $j = j + 1$.

Step 7. Repeat Steps 2–6 for $\mathcal{M}$ iterations to obtain: $\left\{\mathfrak{R}^{(1)}, \mathfrak{R}^{(2)}, \ldots, \mathfrak{R}^{(\mathcal{M})}\right\}$.

Based on the obtained MCMC sample, the Bayes estimate of the stress-strength reliability parameter $\mathfrak{R}$ using the LF-based approach, denoted by $\hat{\mathfrak{R}}_{BLF}$, can be obtained using the approximate posterior mean as follows

$$\hat{\mathfrak{R}}_{BLF} = \frac{1}{\mathcal{M} - \mathcal{B}} \sum_{j=\mathcal{B}+1}^{\mathcal{M}} \mathfrak{R}^{(j)},$$

where $\mathcal{B}$ refers to the burn-in period. In order to obtain the $100\%(1-\alpha)$ BCI of $\mathfrak{R}$, we first sort the acquired MCMC sample as $\left\{\mathfrak{R}^{[\mathcal{B}+1]} < \mathfrak{R}^{[2]} < \ldots < \mathfrak{R}^{[\mathcal{M}]}\right\}$. Then, get the $100\%(1-\alpha)$ BCI bounds as follows

$$\left\{\mathfrak{R}^{[\alpha(\mathcal{M}-\mathcal{B})/2]}, \mathfrak{R}^{[(1-\alpha/2)(\mathcal{M}-\mathcal{B})]}\right\}.$$

Utilizing the second form of the posterior distribution, derived using the SF-based approach, we can derive the full conditional distributions of the model parameters μ_1, μ_2 and β can be derived, respectively, as

$$W_2(\mu_1|\boldsymbol{\theta}_{-\mu_1}, \underline{\mathbf{x}}, \underline{\mathbf{y}}) \propto \mu_1^{\epsilon_1 - 1} \exp\left\{\sum_{i=1}^{d+1} \omega(x_i; \mu_1, \beta) - \mu_1 \varphi(\underline{\mathbf{x}}; \beta)\right\}, \tag{27}$$

$$W_2(\mu_2|\boldsymbol{\theta}_{-\mu_2}, \underline{\mathbf{x}}, \underline{\mathbf{y}}) \propto \mu_2^{\epsilon_2 - 1} \exp\left\{\sum_{i=1}^{q+1} \nu(y_i; \mu_2, \beta) - \mu_2 \psi(\underline{\mathbf{y}}; \beta)\right\}, \tag{28}$$

and

$$W_2(\beta|\boldsymbol{\theta}_{-\beta}, \underline{\mathbf{x}}, \underline{\mathbf{y}}) \propto \beta^{\epsilon_3 - 1} \exp\left\{\sum_{i=1}^{d+1} \omega(x_i; \mu_1, \beta) - \mu_1 \varphi(\underline{\mathbf{x}}; \beta) + \sum_{i=1}^{q+1} \nu(y_i; \mu_2, \beta) - \mu_2 \psi(\underline{\mathbf{y}}; \beta) - \varepsilon_3 \beta\right\}. \tag{29}$$

It is evident from (27) and (29) that the three full conditional distributions do not correspond to any standard distribution. Consequently, we employ the M-H algorithm, as discussed in step 2 in Algorithm 1, to generate the required MCMC samples, using a normal proposal distribution for each parameter. The following steps outline the sample generation process (Algorithm 2):

Algorithm 2: MCMC sample generation using SF

Step 1. Put $j = 1$ and $\left(\mu_1^{(0)}, \mu_2^{(0)}, \beta^{(0)}\right)$, using the MPSEs as beginning values.
Step 2. Generate $\mu_1^{(j)}$ using the M-H algorithm from (27).
Step 3. Simulate $\mu_2^{(j)}$ using the M-H algorithm from (28).
Step 4. Obtain $\beta^{(j)}$ using the M-H algorithm from (29).
Step 5. Calculate $\mathfrak{R}$ at iteration j as:

$$\mathfrak{R}^{*(j)} = \frac{\mu_1^{(j)}}{\mu_1^{(j)} + \mu_2^{(j)}}.$$

Step 6. Set $j = j + 1$.
Step 7. Repeat Steps 2–6 for $\mathcal{M}$ times to get:

$$\left\{\mathfrak{R}^{*(1)}, \mathfrak{R}^{*(2)}, \ldots, \mathfrak{R}^{*(\mathcal{M})}\right\}.$$

After removing a suitable burn-in period, we can calculate the Bayes estimate of the stress-strength reliability parameter $\mathfrak{R}$ employing the SF-based approach, denoted by $\tilde{\mathfrak{R}}_{BSF}$, as follows

$$\tilde{\mathfrak{R}}_{BSF} = \frac{1}{\mathcal{M} - \mathcal{B}} \sum_{j=\mathcal{B}+1}^{\mathcal{M}} \mathfrak{R}^{*(j)}.$$

After sorting the acquired MCMC sample as $\left\{\mathfrak{R}^{*[\mathcal{B}+1]} < \mathfrak{R}^{*[2]} < \ldots < \mathfrak{R}^{*[\mathcal{M}]}\right\}$, we can compute the $100\%(1-\alpha)$ BCI of the stress-strength reliability parameter $\mathfrak{R}$ as

$$\left\{\mathfrak{R}^{*[\alpha(\mathcal{M}-\mathcal{B})/2]}, \mathfrak{R}^{[*(1-\alpha/2)(\mathcal{M}-\mathcal{B})]}\right\}.$$

5 Numerical Comparisons

The purpose of this section is threefold: (i) to examine the finite-sample performance of the proposed estimator under different censoring levels, (ii) to compare its accuracy and robustness against commonly used methods, and (iii) to demonstrate conditions under which our approach provides tangible advantages. Accordingly, this section provides a comprehensive Monte Carlo simulation study to assess the effectiveness and validity of the proposed point and interval estimators for μ_i $(i = 1, 2)$, β, and the stress–strength reliability measure $\mathfrak{R}$, as developed in the preceding discussion. This simulation framework provides a robust platform to investigate the performance of the proposed estimation procedures under realistic censoring levels and different parameter settings.

To establish this goal, a total of 1000 independent UHC samples are drawn from two distinct populations, namely We(μ_1, μ_2, β) distribution, defined respectively as: Set-A: $We(0.5, 1.5, 0.5)$ and Set-B: $We(1, 2, 1)$. For the purposes of this analysis, the true value of the stress-strength reliability index $\mathfrak{R}$ is taken to be $1/4$ and $1/3$ for Set-A and Set-B, respectively. The simulation design incorporates several configurations for the observed UHC sample of size d drawn from n units (k, r, and T_i, $i = 1, 2$) as well as for the other observed UHC sample of size q drawn from m units (k^*, r^*, and T_i^*, $i = 1, 2$).

Now, to generate a UHC dataset, do:

Step 1: Set the true values $We(\mu_1, \beta)$ population.

Step 2: Simulate U_i, $i = 1, 2, \ldots, n$, independent random variables from uniform $U(0, 1)$ distribution.

Step 3: Simulate complete order statistics as:

$$X_i = \left[-\frac{1}{\mu_1}\log(1-u_i)\right]^{\frac{1}{\beta}}, \quad i = 1, 2, \ldots, n.$$

Step 4: Set the desired effective sample sizes r and k

Step 5: Find a and b at T_i (for $i = 1, 2$).

Step 6. Stop and identify the UHC data type as:

a. Stop the test at a at $0 < X_{r:n} < X_{k:n} < T_1$, Case 1;

b. Stop the test at k at $0 < X_{r:n} < T_1 < X_{k:n}$ (or $0 < T_1 < X_{r:n} < X_{k:n}$), Cases 2 and 4;

c. Stop the test at b at $0 < X_{r:n} < T_1 < T_2$ (or $0 < T_1 < X_{r:n} < T_2$), Cases 3 and 5;

d. Stop the test at r at $0 < T_1 < T_2 < X_{r:n}$, Case 6.

d. **Step 7:** Redo Steps 1–6 for $We(\mu_2, \beta)$ population.

To develop the Bayesian estimations of μ_i $(i = 1, 2)$, β, or $\mathfrak{R}$, we consider two informative gamma priors for $(\epsilon_i, \varepsilon_i)$, $i = 1, 2$. Firstly, without loss of generality, we are fixing $(\epsilon_3, \varepsilon_3) = (1,2)$ and (1,1) for Set-A and Set-B, respectively, for the parameter β. Following the past samples algorithm discussed in Nassar and Elshahhat [30], the hyperparameter values for $(\epsilon_1, \epsilon_2, \varepsilon_1, \varepsilon_2)$ of μ_i, $i = 1, 2$, are obtained from the LF and SF approaches, namely:

- For Set-A: $We(0.5, 1.5, 0.5)$:
  - From LF: $(\epsilon_1, \epsilon_2, \varepsilon_1, \varepsilon_2) = (75.7121, 77.8578, 147.3832, 50.4344)$;
  - From SF: $(\epsilon_1, \epsilon_2, \varepsilon_1, \varepsilon_2) = (73.0298, 75.6217, 134.1668, 46.3773)$.
- For Set-B: $We(1, 2, 1)$:
  - From LF: $(\epsilon_1, \epsilon_2, \varepsilon_1, \varepsilon_2) = (75.7139, 77.8583, 73.6933, 37.8260)$;
  - From SF: $(\epsilon_1, \epsilon_2, \varepsilon_1, \varepsilon_2) = (73.0303, 75.6225, 67.0839, 34.7833)$.

To assess the impact of hyperparameter choices on the posterior estimates of the unknown stress-strength reliability, Fig. 2 displays histograms along with their corresponding Gaussian kernel density estimates. These plots are generated under three different configurations for $(\epsilon_i, \varepsilon_i)$, $i = 1, 2, 3$, of μ_i $(i = 1, 2)$, β, each varied by significance more/less the true prior mean; namely:

- For Set-A: $We(0.5, 1.5, 0.5)$ when $\varepsilon_i = 4$, $i = 1, 2, 3$:
  - Prior-A: $(\epsilon_1, \epsilon_2, \epsilon_3) = (3, 8, 3)$;
  - Prior-B: $(\epsilon_1, \epsilon_2, \epsilon_3) = (2, 6, 2)$;
  - Prior-C: $(\epsilon_1, \epsilon_2, \epsilon_3) = (1, 4, 1)$,
- For Set-B: $We(1, 2, 1)$:
  - Prior-A: $(\epsilon_1, \epsilon_2, \epsilon_3) = (6, 10, 6)$;
  - Prior-B: $(\epsilon_1, \epsilon_2, \epsilon_3) = (4, 8, 4)$;
  - Prior-C: $(\epsilon_1, \epsilon_2, \epsilon_3) = (3, 6, 3)$.

After gathering 1000 UCS samples, the 'maxLik' programming, proposed by Henningsen and Toomet [31], is used to produce the MLEs/MPSEs and their 95% ACI estimates of μ_i $(i = 1, 2)$, β, and $\mathfrak{R}$. After installing the 'coda' package (proposed by Plummer et al. [32]), the Bayes point estimations (from LF-based and SF-based) and associated 95% BCI estimations of the same unknown quantities are computed after ignoring the first 2000 MCMC iterations (burn-in) from the total $\mathcal{M} = 12,000$ iterations.

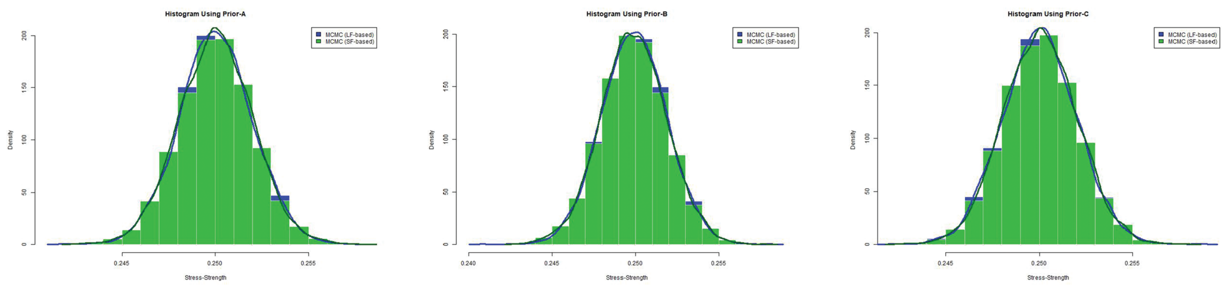

(a) Set–A

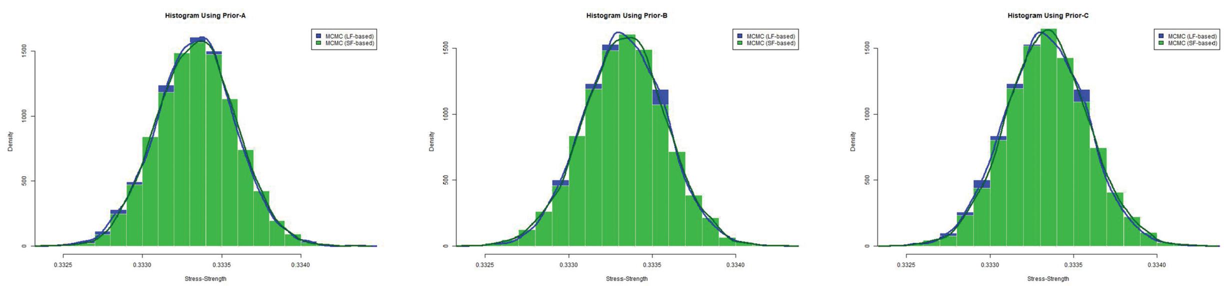

(b) Set–B

Figure 2: Histograms for MCMC iterations of $\mathfrak{R}$ based on three prior sets

In the simulation framework, the average estimated (Av.E) values of the proposed point estimators for the parameter $\mathfrak{R}$ (as an example) are computed as follows:

$$\text{Av.E}\check{\mathfrak{R}} = \frac{1}{1000}\sum_{i=1}^{1000}\check{\mathfrak{R}}^{[i]},$$

where each $\check{\mathfrak{R}}^{[i]}$ corresponds to the ith realization of the estimator based on simulated data.

To assess the quality of these point estimators, we evaluate their accuracy using the rout mean squared error (RMSE) and the average relative absolute bias (ARAB), given respectively by:

$$\text{RMSE}(\check{\mathfrak{R}}) = \sqrt{\frac{1}{1000}\sum_{i=1}^{1000}\left(\check{\mathfrak{R}}^{[i]} - \mathfrak{R}\right)^2},$$

$$\text{ARAB}(\check{\mathfrak{R}}) = \frac{1}{1000}\sum_{i=1}^{1000}\mathfrak{R}^{-1}\left|\check{\mathfrak{R}}^{[i]} - \mathfrak{R}\right|.$$

For interval estimation, performance is quantified through the average interval length (AIL) and the empirical coverage probability (CP) at the nominal 95% confidence level. These are formulated as:

$$\text{AIL}^{95\%}(\mathfrak{R}) = \frac{1}{1000}\sum_{i=1}^{1000}\left(U_{\check{\mathfrak{R}}^{[i]}} - L_{\check{\mathfrak{R}}^{[i]}}\right),$$

$$\mathrm{CP}^{95\%}(\mathfrak{R}) = \frac{1}{1000}\sum_{i=1}^{1000}\mathbb{D}_{\left(L_{\hat{\mathfrak{R}}[i]},U_{\hat{\mathfrak{R}}[i]}\right)}(\mathfrak{R}),$$

where $\mathbb{D}(\cdot)$ denotes the indicator function, and $L(\cdot)$ and $U(\cdot)$ represent the lower and upper bounds of the associated 95% credible or confidence intervals for $\mathfrak{R}$.

Tables 1–4 detail the Av.Es, RMSEs, and ARABs across their respective columns, while Tables 5 and 6 report the AILs and CPs. A comprehensive evaluation of Tables 1–8 reveals several notable observations, especially when considering estimators that achieve the smallest RMSEs, ARABs, and AILs along with the highest CPs:

Table 1: Point estimation results when $(T_1, T_2) = (T_1^*, T_2^*) = (0.5, 1.0)$ from Set-A

n	(r,k)	Par.	MLE			MPSE			MCMC					
m	(r^*,k^*)								LF			SF		
20	(5, 8)	μ_1	0.747	0.299	0.504	0.811	0.335	0.627	0.588	0.252	0.346	0.646	0.309	0.415
30	(10, 15)	μ_2	1.639	0.510	0.243	1.973	0.780	0.372	1.676	0.218	0.128	1.618	0.156	0.089
		β	0.637	0.210	0.276	2.332	1.376	2.367	0.454	0.196	0.187	0.831	0.385	0.662
		$\mathfrak{R}$	0.268	0.089	0.328	0.338	0.093	0.351	0.306	0.068	0.223	0.333	0.089	0.333
	(10, 15)	μ_1	0.745	0.283	0.550	0.805	0.329	0.622	0.717	0.213	0.437	0.613	0.232	0.330
	(15, 25)	μ_2	1.634	0.422	0.210	1.870	0.660	0.301	1.676	0.219	0.128	1.614	0.154	0.089
		β	0.462	0.193	0.197	1.504	1.106	2.157	0.510	0.110	0.170	0.732	0.282	0.464
		$\mathfrak{R}$	0.327	0.082	0.309	0.337	0.092	0.347	0.305	0.064	0.220	0.251	0.085	0.270
50	(20, 30)	μ_1	0.762	0.278	0.524	0.804	0.327	0.611	0.573	0.199	0.283	0.639	0.205	0.312
60	(30, 40)	μ_2	1.573	0.280	0.144	2.010	0.626	0.347	1.603	0.149	0.082	1.609	0.151	0.086
		β	0.479	0.168	0.171	1.834	1.070	2.009	0.508	0.071	0.112	0.715	0.267	0.430
		$\mathfrak{R}$	0.263	0.079	0.286	0.336	0.090	0.324	0.309	0.061	0.204	0.251	0.074	0.237
	(30, 40)	μ_1	0.743	0.269	0.490	0.814	0.337	0.608	0.528	0.118	0.178	0.661	0.184	0.324
	(40, 50)	μ_2	1.558	0.240	0.124	1.859	0.591	0.246	1.601	0.154	0.082	1.593	0.130	0.072
		β	0.516	0.168	0.125	1.102	1.034	1.799	0.504	0.066	0.104	0.690	0.246	0.380
		$\mathfrak{R}$	0.322	0.076	0.279	0.328	0.087	0.312	0.253	0.050	0.161	0.243	0.053	0.171
90	(50, 60)	μ_1	0.716	0.239	0.441	0.793	0.319	0.585	0.522	0.090	0.136	0.635	0.177	0.285
80	(40, 50)	μ_2	1.552	0.229	0.118	1.980	0.579	0.325	1.515	0.094	0.039	1.576	0.114	0.062
		β	0.495	0.162	0.097	1.508	0.627	1.204	0.502	0.057	0.090	0.647	0.204	0.296
		$\mathfrak{R}$	0.321	0.071	0.249	0.328	0.085	0.314	0.250	0.036	0.116	0.253	0.040	0.128
	(70, 80)	μ_1	0.512	0.068	0.105	0.791	0.311	0.581	0.510	0.050	0.078	0.601	0.118	0.206
	(60, 70)	μ_2	1.536	0.169	0.089	1.862	0.418	0.244	1.500	0.096	0.035	1.566	0.105	0.055
		β	0.452	0.153	0.089	0.804	0.321	0.609	0.499	0.052	0.083	0.514	0.132	0.196
		$\mathfrak{R}$	0.253	0.040	0.128	0.256	0.043	0.137	0.250	0.025	0.080	0.245	0.027	0.085

Table 2: Point estimation results when $(T_1, T_2) = (T_1^*, T_2^*) = (1.5, 2.0)$ from Set-A

n	(r, k)	Par.	MLE			MPSE			MCMC					
m	(r^*, k^*)								LF			SF		
20	(5, 8)	μ_1	0.746	0.286	0.504	0.805	0.379	0.679	0.559	0.192	0.282	0.614	0.258	0.362
30	(10, 15)	μ_2	1.557	0.326	0.167	1.850	0.531	0.273	1.677	0.220	0.129	1.629	0.166	0.096
		β	0.447	0.199	0.201	1.324	0.852	1.648	0.496	0.102	0.159	0.815	0.368	0.630
		$\mathfrak{R}$	0.326	0.081	0.304	0.335	0.090	0.339	0.305	0.061	0.219	0.250	0.077	0.247
	(10, 15)	μ_1	0.744	0.282	0.498	0.811	0.335	0.622	0.557	0.169	0.251	0.616	0.238	0.343
	(15, 25)	μ_2	1.552	0.285	0.147	1.905	0.473	0.273	1.672	0.214	0.125	1.622	0.160	0.094
		β	0.458	0.195	0.180	1.235	0.750	1.469	0.497	0.101	0.157	0.732	0.282	0.464
		$\mathfrak{R}$	0.322	0.076	0.286	0.336	0.092	0.345	0.264	0.062	0.195	0.266	0.070	0.219
50	(20, 30)	μ_1	0.746	0.261	0.493	0.816	0.340	0.632	0.517	0.098	0.152	0.640	0.199	0.308
60	(30, 40)	μ_2	1.548	0.224	0.116	1.827	0.415	0.226	1.603	0.151	0.082	1.612	0.149	0.085
		β	0.503	0.176	0.171	1.203	0.721	1.406	0.502	0.065	0.103	0.711	0.265	0.421
		$\mathfrak{R}$	0.265	0.072	0.268	0.334	0.090	0.338	0.252	0.043	0.136	0.260	0.050	0.158
	(30, 40)	μ_1	0.737	0.256	0.479	0.819	0.342	0.637	0.521	0.088	0.135	0.645	0.188	0.304
	(40, 50)	μ_2	1.528	0.193	0.102	1.833	0.383	0.224	1.617	0.170	0.093	1.589	0.125	0.070
		β	0.500	0.167	0.115	0.961	0.492	0.924	0.502	0.064	0.102	0.676	0.234	0.352
		$\mathfrak{R}$	0.317	0.070	0.246	0.333	0.088	0.332	0.255	0.038	0.119	0.270	0.045	0.142
90	(30, 40)	μ_1	0.716	0.239	0.441	0.796	0.323	0.593	0.512	0.066	0.104	0.661	0.179	0.283
80	(40, 50)	μ_2	1.535	0.190	0.100	1.687	0.342	0.176	1.500	0.096	0.035	1.589	0.127	0.070
		β	0.452	0.162	0.089	0.955	0.472	0.910	0.499	0.053	0.085	0.651	0.208	0.302
		$\mathfrak{R}$	0.306	0.062	0.224	0.328	0.087	0.311	0.251	0.032	0.102	0.259	0.037	0.117
	(70, 80)	μ_1	0.715	0.226	0.431	0.791	0.311	0.581	0.510	0.050	0.078	0.606	0.122	0.214
	(60, 70)	μ_2	1.525	0.158	0.084	1.744	0.316	0.173	1.510	0.092	0.037	1.609	0.151	0.086
		β	0.482	0.154	0.081	0.785	0.300	0.570	0.498	0.052	0.083	0.646	0.204	0.293
		$\mathfrak{R}$	0.307	0.059	0.213	0.328	0.085	0.314	0.251	0.024	0.077	0.249	0.024	0.077

Table 3: Point estimation results when $(T_1, T_2) = (T_1^*, T_2^*) = (0.5, 1.0)$ from Set-B

n	(r, k)	Par.	MLE			MPSE			MCMC					
m	(r^*, k^*)								LF			SF		
20	(5, 8)	μ_1	1.155	0.405	0.286	1.211	0.436	0.308	1.156	0.182	0.159	1.219	0.266	0.259
30	(10, 15)	μ_2	2.191	0.559	0.207	2.569	0.854	0.322	2.151	0.208	0.091	2.076	0.127	0.049
		β	1.112	0.349	0.230	4.060	1.849	3.060	0.967	0.186	0.080	1.283	0.336	0.283
		$\mathfrak{R}$	0.345	0.077	0.187	0.321	0.075	0.177	0.363	0.034	0.091	0.375	0.045	0.125

(Continued)

Table 3 **(continued)**

n / m	(r,k) / (r^*,k^*)	Par.	MLE			MPSE			MCMC LF			MCMC SF		
	(10, 15)	μ_1	1.094	0.310	0.228	1.247	0.428	0.314	1.039	0.179	0.148	1.231	0.249	0.231
	(15, 25)	μ_2	2.082	0.451	0.169	2.613	0.735	0.311	2.152	0.203	0.087	2.058	0.118	0.041
		β	1.017	0.195	0.146	2.559	1.602	1.559	0.971	0.184	0.076	1.251	0.306	0.251
		$\mathfrak{R}$	0.345	0.073	0.175	0.337	0.072	0.173	0.334	0.034	0.082	0.377	0.048	0.131
50	(20, 30)	μ_1	1.155	0.181	0.185	1.264	0.343	0.276	1.136	0.170	0.140	1.215	0.239	0.215
60	(30, 40)	μ_2	2.057	0.315	0.123	2.457	0.705	0.267	2.074	0.140	0.050	2.047	0.107	0.034
		β	1.022	0.166	0.104	2.927	1.959	1.927	0.990	0.159	0.051	1.159	0.244	0.186
		$\mathfrak{R}$	0.337	0.049	0.117	0.327	0.049	0.119	0.359	0.030	0.078	0.369	0.041	0.106
	(30, 40)	μ_1	1.137	0.171	0.161	1.247	0.323	0.260	1.033	0.167	0.129	1.204	0.222	0.204
	(40, 50)	μ_2	2.056	0.301	0.117	2.590	0.685	0.297	2.073	0.139	0.049	2.048	0.106	0.034
		β	1.016	0.159	0.093	2.462	1.493	1.462	1.000	0.151	0.043	1.159	0.215	0.162
		$\mathfrak{R}$	0.336	0.047	0.112	0.330	0.048	0.114	0.358	0.028	0.075	0.370	0.042	0.110
90	(30, 40)	μ_1	1.161	0.169	0.142	1.315	0.354	0.317	1.156	0.146	0.084	1.198	0.220	0.198
80	(40, 50)	μ_2	2.048	0.273	0.106	2.540	0.658	0.275	1.988	0.095	0.023	2.030	0.096	0.026
		β	1.007	0.148	0.085	2.897	1.918	1.897	0.984	0.141	0.056	1.114	0.174	0.115
		$\mathfrak{R}$	0.367	0.040	0.103	0.368	0.044	0.110	0.345	0.018	0.037	0.338	0.039	0.093
	(70, 80)	μ_1	1.019	0.156	0.128	1.221	0.256	0.224	1.016	0.121	0.095	1.196	0.213	0.196
	(60, 70)	μ_2	2.046	0.238	0.095	2.435	0.524	0.222	1.981	0.094	0.021	2.032	0.094	0.026
		β	1.007	0.139	0.072	1.858	0.884	0.858	0.968	0.125	0.069	1.107	0.170	0.108
		$\mathfrak{R}$	0.368	0.038	0.100	0.369	0.041	0.107	0.345	0.017	0.037	0.335	0.036	0.086

Table 4: Point estimation results when $(T_1, T_2) = (T_1^*, T_2^*) = (1.5, 2.0)$ from Set-B

n / m	(r,k) / (r^*,k^*)	Par.	MLE			MPSE			MCMC LF			MCMC SF		
20	(5, 8)	μ_1	1.066	0.243	0.188	1.130	0.308	0.232	1.129	0.163	0.135	1.229	0.247	0.229
30	(10, 15)	μ_2	2.057	0.336	0.133	2.163	0.375	0.145	2.152	0.205	0.087	2.030	0.094	0.026
		β	0.958	0.190	0.126	1.525	0.537	0.525	1.006	0.156	0.088	1.225	0.280	0.225
		$\mathfrak{R}$	0.342	0.060	0.145	0.342	0.064	0.154	0.337	0.039	0.092	0.377	0.049	0.135
	(10, 15)	μ_1	1.072	0.243	0.186	1.121	0.289	0.221	1.164	0.190	0.167	1.224	0.248	0.224
	(15, 25)	μ_2	2.061	0.333	0.132	2.153	0.372	0.144	2.152	0.204	0.087	2.030	0.094	0.026
		β	0.960	0.189	0.125	1.489	0.505	0.489	1.008	0.146	0.087	1.200	0.256	0.200
		$\mathfrak{R}$	0.342	0.059	0.143	0.342	0.062	0.150	0.334	0.031	0.075	0.377	0.047	0.130
50	(20, 30)	μ_1	1.163	0.183	0.147	1.223	0.245	0.220	1.023	0.164	0.134	1.168	0.245	0.191
60	(30, 40)	μ_2	2.028	0.231	0.090	2.228	0.335	0.132	2.082	0.165	0.065	2.070	0.122	0.045
		β	0.995	0.165	0.108	1.441	0.460	0.441	1.009	0.137	0.052	1.139	0.201	0.142
		$\mathfrak{R}$	0.370	0.041	0.111	0.344	0.049	0.128	0.355	0.026	0.064	0.368	0.041	0.112

(Continued)

Table 4 (continued)

n	(r,k)	Par.	MLE			MPSE			MCMC					
m	(r^*,k^*)								LF			SF		
	(30, 40)	μ_1	1.132	0.167	0.142	1.228	0.242	0.218	1.027	0.142	0.110	1.159	0.231	0.181
	(40, 50)	μ_2	2.029	0.229	0.090	2.227	0.336	0.133	2.084	0.151	0.055	2.070	0.122	0.046
		β	0.989	0.162	0.084	1.420	0.459	0.420	1.008	0.127	0.047	1.125	0.190	0.128
		$\mathfrak{R}$	0.370	0.040	0.110	0.371	0.045	0.118	0.353	0.024	0.058	0.343	0.042	0.098
90	(30, 40)	μ_1	1.142	0.148	0.138	1.192	0.232	0.197	1.133	0.139	0.133	1.210	0.228	0.210
80	(40, 50)	μ_2	2.027	0.199	0.080	2.244	0.323	0.133	1.976	0.093	0.023	2.076	0.126	0.049
		β	0.975	0.147	0.069	1.387	0.430	0.389	1.001	0.088	0.061	1.090	0.160	0.092
		$\mathfrak{R}$	0.336	0.039	0.094	0.371	0.044	0.112	0.345	0.017	0.035	0.347	0.036	0.084
	(70, 80)	μ_1	1.015	0.105	0.082	1.204	0.222	0.204	1.014	0.098	0.078	1.163	0.198	0.168
	(60, 70)	μ_2	2.029	0.197	0.079	2.241	0.325	0.133	1.979	0.091	0.021	2.075	0.125	0.048
		β	0.979	0.125	0.066	1.380	0.394	0.380	1.002	0.085	0.058	1.088	0.159	0.089
		$\mathfrak{R}$	0.334	0.030	0.072	0.369	0.040	0.106	0.344	0.016	0.033	0.342	0.032	0.075

Table 5: Interval estimation results when $(T_1, T_2) = (T_1^*, T_2^*) = (0.5, 1.0)$ from Set-A

n	(r,k)	Par.	ACI				BCI			
m	(r^*,k^*)		LF		SF		LF		SF	
20	(5, 8)	μ_1	0.807	0.933	0.888	0.926	0.455	0.962	0.472	0.961
30	(10, 15)	μ_2	1.758	0.853	1.938	0.838	0.345	0.971	0.457	0.962
		β	0.468	0.961	1.442	0.880	0.438	0.964	0.595	0.950
		$\mathfrak{R}$	0.271	0.977	0.326	0.973	0.091	0.992	0.120	0.990
	(10, 15)	μ_1	0.639	0.947	0.662	0.945	0.433	0.964	0.447	0.963
	(15, 25)	μ_2	1.506	0.875	1.643	0.863	0.324	0.973	0.428	0.964
		β	0.437	0.964	1.225	0.898	0.411	0.966	0.549	0.954
		$\mathfrak{R}$	0.227	0.981	0.253	0.979	0.090	0.993	0.119	0.990
50	(20, 30)	μ_1	0.421	0.965	0.463	0.961	0.344	0.971	0.403	0.966
60	(30, 40)	μ_2	1.033	0.914	1.205	0.900	0.327	0.973	0.361	0.970
		β	0.376	0.969	1.059	0.912	0.282	0.976	0.507	0.958
		$\mathfrak{R}$	0.193	0.984	0.168	0.986	0.073	0.994	0.118	0.990
	(30, 40)	μ_1	0.328	0.973	0.439	0.963	0.318	0.974	0.390	0.968
	(40, 50)	μ_2	0.827	0.931	0.957	0.920	0.295	0.975	0.328	0.973
		β	0.385	0.968	0.698	0.942	0.256	0.979	0.424	0.965
		$\mathfrak{R}$	0.150	0.988	0.150	0.987	0.061	0.995	0.107	0.991
90	(30, 40)	μ_1	0.286	0.976	0.413	0.966	0.259	0.978	0.368	0.969
80	(40, 50)	μ_2	0.886	0.926	1.049	0.913	0.270	0.977	0.293	0.976
		β	0.327	0.973	0.634	0.947	0.214	0.982	0.412	0.966
		$\mathfrak{R}$	0.121	0.990	0.132	0.989	0.098	0.992	0.103	0.991

(Continued)

Table 5 (continued)

n	(r, k)	Par.	ACI				BCI			
m	(r^*, k^*)		LF		SF		LF		SF	
	(70, 80)	μ_1	0.236	0.980	0.342	0.971	0.193	0.984	0.224	0.981
	(60, 70)	μ_2	0.633	0.947	0.756	0.937	0.257	0.979	0.279	0.977
		β	0.288	0.976	0.540	0.955	0.200	0.983	0.307	0.974
		$\mathfrak{R}$	0.097	0.992	0.117	0.990	0.087	0.993	0.097	0.992

Table 6: Interval estimation results when $(T_1, T_2) = (T_1^*, T_2^*) = (1.5, 2.0)$ from Set-A

n	(r, k)	Par.	ACI				BCI			
m	(r^*, k^*)		LF		SF		LF		SF	
20	(5,8)	μ_1	0.669	0.944	0.735	0.939	0.464	0.961	0.497	0.959
30	(10, 15)	μ_2	1.272	0.894	1.471	0.877	0.333	0.972	0.431	0.964
		β	0.497	0.959	1.020	0.915	0.387	0.968	0.671	0.944
		$\mathfrak{R}$	0.274	0.977	0.262	0.978	0.089	0.993	0.137	0.989
	(10, 15)	μ_1	0.590	0.951	0.674	0.944	0.432	0.964	0.477	0.960
	(15, 25)	μ_2	1.062	0.912	1.163	0.903	0.319	0.973	0.423	0.965
		β	0.486	0.959	0.699	0.942	0.376	0.969	0.584	0.951
		$\mathfrak{R}$	0.235	0.980	0.247	0.979	0.094	0.992	0.122	0.990
50	(20, 30)	μ_1	0.370	0.969	0.448	0.963	0.377	0.969	0.414	0.966
60	(30, 40)	μ_2	0.821	0.932	0.930	0.922	0.294	0.976	0.406	0.966
		β	0.414	0.966	0.602	0.950	0.259	0.978	0.542	0.955
		$\mathfrak{R}$	0.164	0.986	0.166	0.986	0.068	0.994	0.118	0.990
	(30, 40)	μ_1	0.344	0.971	0.400	0.967	0.275	0.977	0.395	0.967
	(40, 50)	μ_2	0.727	0.939	0.819	0.932	0.289	0.976	0.366	0.969
		β	0.377	0.969	0.490	0.959	0.253	0.979	0.484	0.960
		$\mathfrak{R}$	0.142	0.988	0.151	0.987	0.063	0.995	0.111	0.991
90	(30, 40)	μ_1	0.326	0.973	0.342	0.971	0.221	0.982	0.326	0.973
80	(40, 50)	μ_2	0.730	0.939	0.867	0.928	0.288	0.976	0.335	0.972
		β	0.368	0.969	0.460	0.962	0.206	0.983	0.429	0.964
		$\mathfrak{R}$	0.126	0.990	0.143	0.988	0.097	0.992	0.103	0.991
	(70, 80)	μ_1	0.254	0.979	0.313	0.974	0.193	0.984	0.226	0.981
	(60, 70)	μ_2	0.610	0.949	0.725	0.940	0.282	0.976	0.324	0.973
		β	0.339	0.972	0.430	0.964	0.200	0.983	0.402	0.966
		$\mathfrak{R}$	0.095	0.992	0.121	0.990	0.087	0.993	0.110	0.990

Table 7: Interval estimation results when $(T_1, T_2) = (T_1^*, T_2^*) = (0.5, 1.0)$ from Set-B

n	(r, k)	Par.	ACI				BCI			
m	(r^*, k^*)		LF		SF		LF		SF	
20	(5, 8)	μ_1	1.259	0.895	1.394	0.884	0.337	0.972	0.366	0.969
30	(10, 15)	μ_2	1.958	0.837	2.102	0.825	0.433	0.964	0.492	0.959
		β	1.098	0.909	1.850	0.846	0.458	0.962	0.643	0.946
		$\mathfrak{R}$	0.286	0.976	0.290	0.976	0.066	0.994	0.086	0.993
	(10, 15)	μ_1	1.073	0.911	1.128	0.906	0.324	0.973	0.351	0.971
	(15, 25)	μ_2	1.680	0.860	1.846	0.846	0.413	0.966	0.451	0.962
		β	0.731	0.939	1.784	0.851	0.454	0.962	0.614	0.949
		$\mathfrak{R}$	0.228	0.981	0.254	0.979	0.060	0.995	0.082	0.993
50	(20, 30)	μ_1	0.662	0.945	0.714	0.940	0.312	0.974	0.332	0.972
60	(30, 40)	μ_2	1.174	0.902	1.339	0.888	0.367	0.969	0.428	0.964
		β	0.513	0.957	1.679	0.860	0.365	0.970	0.486	0.960
		$\mathfrak{R}$	0.185	0.985	0.215	0.982	0.045	0.996	0.075	0.994
	(30, 40)	μ_1	0.632	0.947	0.692	0.942	0.226	0.981	0.313	0.974
	(40, 50)	μ_2	1.117	0.907	1.265	0.895	0.365	0.970	0.381	0.968
		β	0.476	0.960	1.265	0.895	0.366	0.970	0.439	0.963
		$\mathfrak{R}$	0.179	0.985	0.195	0.984	0.047	0.996	0.071	0.994
90	(30, 40)	μ_1	0.473	0.961	0.546	0.955	0.186	0.984	0.285	0.976
80	(40, 50)	μ_2	1.021	0.915	1.139	0.905	0.285	0.976	0.296	0.975
		β	0.400	0.967	1.089	0.909	0.369	0.969	0.398	0.967
		$\mathfrak{R}$	0.148	0.988	0.162	0.986	0.046	0.996	0.071	0.994
	(70, 80)	μ_1	0.414	0.966	0.470	0.961	0.159	0.987	0.263	0.978
	(60, 70)	μ_2	0.903	0.925	1.018	0.915	0.269	0.978	0.293	0.976
		β	0.348	0.971	0.660	0.945	0.361	0.970	0.385	0.968
		$\mathfrak{R}$	0.133	0.989	0.152	0.987	0.042	0.997	0.067	0.994

Table 8: Interval estimation results when $(T_1, T_2) = (T_1^*, T_2^*) = (1.5, 2.0)$ from Set-B

n	(r, k)	Par.	ACI				BCI			
m	(r^*, k^*)		LF		SF		LF		SF	
20	(5, 8)	μ_1	0.913	0.924	0.992	0.917	0.328	0.973	0.343	0.971
30	(10, 15)	μ_2	1.283	0.893	1.363	0.886	0.388	0.968	0.485	0.960
		β	0.614	0.949	0.871	0.927	0.472	0.961	0.547	0.954
		$\mathfrak{R}$	0.235	0.980	0.240	0.980	0.064	0.995	0.081	0.993

(Continued)

Table 8 (continued)

n	(r,k)	Par.	ACI				BCI			
m	(r^*,k^*)		LF		SF		LF		SF	
	(10, 15)	μ_1	0.899	0.925	0.964	0.920	0.274	0.977	0.337	0.972
	(15, 25)	μ_2	1.281	0.893	1.354	0.887	0.299	0.975	0.437	0.964
		β	0.613	0.949	0.844	0.930	0.468	0.961	0.509	0.958
		$\mathfrak{R}$	0.232	0.981	0.236	0.980	0.062	0.995	0.078	0.994
50	(20, 30)	μ_1	0.557	0.954	0.630	0.948	0.253	0.979	0.273	0.977
60	(30, 40)	μ_2	0.895	0.925	0.969	0.919	0.286	0.976	0.386	0.968
		β	0.415	0.965	0.614	0.949	0.387	0.968	0.465	0.961
		$\mathfrak{R}$	0.155	0.987	0.156	0.987	0.059	0.995	0.072	0.994
	(30, 40)	μ_1	0.541	0.955	0.607	0.949	0.214	0.982	0.278	0.977
	(40, 50)	μ_2	0.893	0.926	0.972	0.919	0.269	0.978	0.299	0.975
		β	0.413	0.966	0.587	0.951	0.369	0.969	0.450	0.963
		$\mathfrak{R}$	0.152	0.987	0.153	0.987	0.054	0.995	0.071	0.994
90	(30, 40)	μ_1	0.412	0.966	0.475	0.960	0.174	0.986	0.317	0.974
80	(40, 50)	μ_2	0.773	0.936	0.838	0.930	0.256	0.979	0.287	0.976
		β	0.354	0.971	0.518	0.957	0.326	0.973	0.368	0.969
		$\mathfrak{R}$	0.124	0.990	0.124	0.990	0.048	0.996	0.067	0.994
	(70, 80)	μ_1	0.379	0.968	0.433	0.964	0.157	0.987	0.306	0.974
	(60, 70)	μ_2	0.770	0.936	0.844	0.930	0.248	0.979	0.283	0.976
		β	0.326	0.973	0.445	0.963	0.313	0.974	0.366	0.969
		$\mathfrak{R}$	0.117	0.990	0.119	0.990	0.046	0.996	0.066	0.995

- The proposed estimation procedures for the Weibull distribution parameters under stress-strength (including $\mu_i, i = 1, 2, \beta$, and $\mathfrak{R}$) generally demonstrate reliable inferential accuracy.
- Bayesian estimators derived via MCMC methods consistently outperform their competitive classical approaches. This performance gain arises from the Bayesian paradigm's utilization of prior information in addition to censored data, unlike likelihood-based techniques that rely exclusively on observed samples.
- The BCIs outperformed ACIs due to their prior knowledge of the parameters under investigation. They consistently yielded narrower intervals and better empirical coverage across all assessed parameters.
- An increase in n (or m) improves the estimation precision. Similar improvements are noted as both d and q increase simultaneously.
- Increasing the threshold limits of $T_i,\ i = 1, 2$ (or $T_i^*,\ i = 1, 2$), the accuracy of inferential outcomes for all considered parameters becomes better by reducing their simulated RRMSE, ARAB, and AIL values and increasing their simulated CP values.
- When the true parameter values $\mu_i, i = 1, 2$, and β increase:
  – The RMSEs and ARABs for $\mu_i, i = 1, 2$ tend to decrease in the case of Bayes outcomes from the Lf-based (or SF-based) approach and tend to increase for the frequentist outcomes from the LF (or SF) approach.

- The RMSEs and ARABs for β and $\Re$ decreased in most cases for all point estimation setups.
- The AILs associated with $\mu_i, i = 1, 2$ and β tend to increase for all interval estimation approaches, while those of $\Re$ decreased.
- The CPs associated with $\mu_i, i = 1, 2$ and β tend to decrease, while those of $\Re$ increase for all interval estimation approaches.

- Comparing the point and interval estimation strategies, for all unknown parameters $\mu_i, i = 1, 2$, β, and $\Re$, it is noted that:
  - The ML method outperformed the MPS method;
  - The Bayes method (LF-based) outperformed its competitor using SF-based;
  - The ACI (LF-based) method outperformed the ACI (SF-based) method;
  - The BCI method (LF-based) outperformed its competitor using the SF-based.
- In conclusion, the MCMC inference using LF-based is now recommended for We parameter estimation and its stress-strength reliability metric when a dataset under investigation is gathered from UHC settings.

Across all scenarios, the Bayesian method consistently exhibited lower bias and mean squared error than the frequentist method. This finding underscores the practical significance of our approach: in applied survival studies, where censoring is common, the improved reliability of estimates can substantially strengthen inference. The comparisons confirm that the proposed methods preserve efficiency under light censoring while remaining robust under heavier censoring. These properties make the approach particularly appealing for practitioners who require reliable inference across a wide range of data conditions. Thus, the simulations not only corroborate the theoretical properties but also demonstrate the method's practical utility in real-world applications.

6 LED Data Analysis

The LED is a solid-state semiconductor product that generates visible or infrared light when exposed to an electrical current. Among recent advancements, organic white LEDs (WOLEDs) have garnered significant attention due to their potential for energy-efficient, cost-effective lighting solutions. WOLEDs are particularly notable for their ability to produce high-quality white light over broad emitting surfaces. In the context of reliability analysis, the lifetime performance of these devices is a critical factor, especially under varying environmental and operational stresses; see Farinola and Ragni [33]. This study focuses on the M00071 series of WOLEDs, which incorporates red, green, and blue organic emitters under two stress levels, namely: 9.64 mA (with $n = 10$) and 17.09 mA (with $m = 10$). This data set was originally reported by Zhang et al. [34]. For calculation purposes, in Table 9, each data point has been divided by a thousand for computational purposes.

Table 9: Failure times in WOLED datasets

Group	Data									
X (9.64 mA)	1.6915	2.0847	2.1003	2.3745	2.4215	2.5860	2.6215	2.6805	2.8680	2.8795
Y (17.09 mA)	0.6015	0.6897	0.6973	0.7165	0.7855	0.8545	0.8895	1.1157	1.1313	1.2515

Using the ML estimation, the shape parameter β is estimated as 8.54 (95% ACI-LF as [5.13, 14.23]). Since the confidence interval excludes 1, this indicates that the hazard is not constant but increases with time. This step provides clarity regarding the underlying distributional form of the WOLEDs data. Having established the behavior of the shape parameter β, we then proceeded with the goodness-of-fit assessment. Fig. 3 compares the fitted Weibull survival curve (blue) with the nonparametric Kaplan-Meier estimate (red). The fitted Weibull curve closely follows the Kaplan-Meier trajectory, and its 95% confidence band comfortably covers the empirical survival function. Additionally, the model's Akaike information criterion (AIC) value of 10.87 further supports its adequacy.

Following the benefits and importance of WOLEDs in life today and to demonstrate the utility of our proposed statistical methodologies, we analyze lifetime data obtained under two predefined stress conditions. To evaluate the suitability of the We distribution in modeling the WOLED datasets, we first compute the MLEs of $\mu_i,\ i = 1, 2$ and β, along with their corresponding standard errors (SEs). Additionally, to further assess the precision of the estimates, we calculate the 95% ACIs for the same unknown coefficients, including their respective interval lengths (ILs). These parameter estimates are subsequently utilized to compute the Kolmogorov-Smirnov (KS) test statistic and its associated p-value, see Table 10. Since the observed p-value notably exceeds the conventional significance level of $\alpha = 0.05$, we conclude that the We distribution offers an adequate fit to the WOLED datasets.

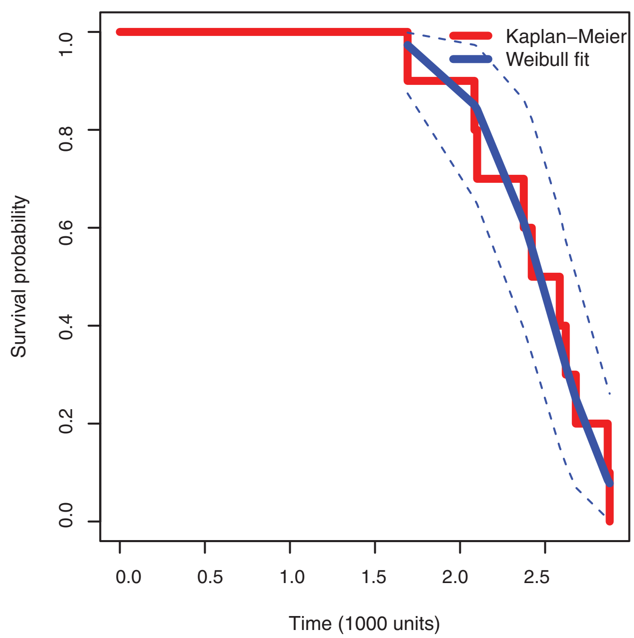

Figure 3: Fitted Weibull survival curve vs. the Kaplan-Meier estimate from the WOLEDs data

Table 10: Fitting summary of We lifespan model from WOLED datasets

Group	Par.	MLE (SE)	95% ACI			KS (p-Value)
			Low.	Upp.	IW	
X	β	6.4327 (0.5344)	5.3853	7.4801	2.0947	0.1878 (0.8102)
	μ_1	0.0026 (0.0011)	0.0004	0.0048	0.0044	
Y	β	4.4606 (1.0765)	2.3507	6.5704	4.2197	0.1866 (0.8163)
	μ_2	1.2145 (0.3922)	0.4457	1.9832	1.5375	

A comprehensive diagnostic assessment of model fit is provided in Fig. 4, leveraging six complementary graphical tools: (1) fitted We density line with histograms of the WOLED lifetimes; (2) empirical/estimated reliability lines; (3) empirical/estimated probability-probability (PP) lines; (4) empirical/estimated quantile-quantile (QQ) lines; (5) empirical/estimated scaled-TTT lines; and (6) contour map of the log-LF. Under both groups X and Y, visual subplots in Fig. 4a–d consistently indicate strong concordance between the observed data and the fitted We lifetime models. Furthermore, in Fig. 4e, the TTT plots reveal an increasing hazard trend in both datasets, aligning with a key characteristic of the We distribution's failure behavior. Finally, the contour plot in Fig. 4f confirms the existence and uniqueness of the MLEs for the We parameters μ_i ($i = 1, 2$) and β, recommending their appropriateness as initial values in subsequent estimation routines.

Before proceeding, we test whether the shape parameter can be treated as common across the stress and strength populations using a likelihood–ratio (LR) test. The LR statistic is

$$\Delta = 2\left\{\ell_{\text{stress}} + \ell_{\text{strength}} - \ell_c\right\},$$

where ℓ_{stress} and ℓ_{strength} are the maximized log-likelihoods from the separate fits, and ℓ_c is the maximized log-likelihood under the constrained model with a shared shape parameter. Under H_0 (common shape), $\Delta \sim \chi^2_1$. For the WOLED data, $\Delta = 2.137$, which gives a p-value of $p \approx 0.144$. Hence, we do not reject H_0 at conventional significance levels (e.g., 5% or 10%).

To evaluate the derived point and interval estimators for the parameters $\mu_i (i = 1, 2)$, β, and $\mathfrak{R}$ across each WOLED dataset group summarized in Table 9, four synthetic UTIPHC datasets, denoted as $\mathbb{S}[i]$ for $i = 1, 2, 3$, are generated. These samples are constructed under the framework of $r = r^* = 4$ and $k = k^* = 8$, with varying schemes for T_i and T_i^* for ($i = 1, 2$), as detailed in Table 11. For each simulated dataset in Table 11, point estimates (along with their SEs) and 95% interval estimates (accompanied by ILs) are computed for $\mu_i (i = 1, 2)$, β, and $\mathfrak{R}$ using both the developed frequentist and Bayesian techniques (see Table 12).

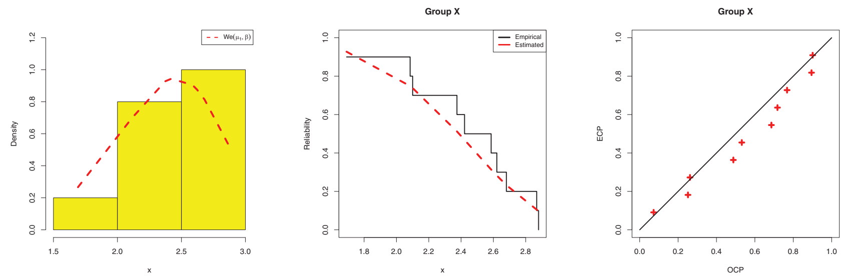

(a) PDF (b) RF (c) PP

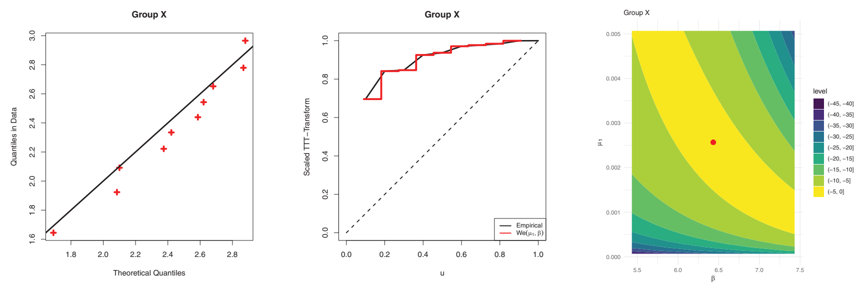

(d) QQ (e) TTT (f) Contour

(i) Group-X

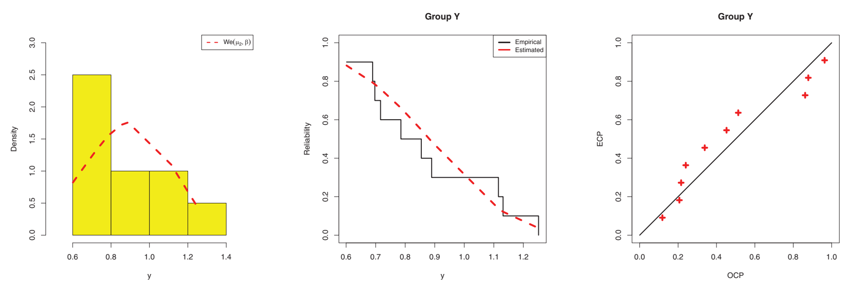

(a) PDF (b) RF (c) PP

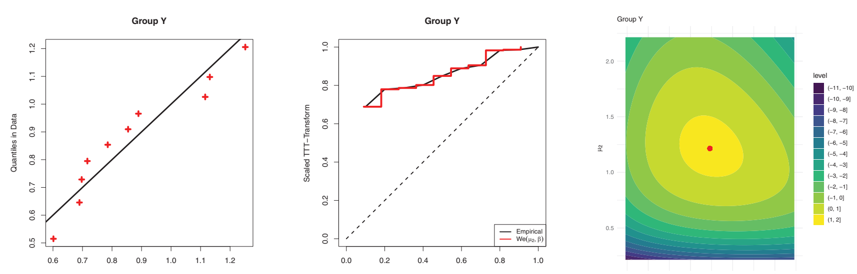

(d) QQ (e) TTT (f) Contour

(ii) Group-Y

Figure 4: Visualization graphs of the We lifespan model from WOLED datasets. (**a**): PDF; (**b**): RF; (**c**): PP; (**d**): QQ; (**e**): TTT; (**f**): Contour

Table 11: Artificial UHC samples from WOLED datasets

Sample	$T_1(a)$ $T_1^*(a^*)$	$T_2(b)$ $T_2^*(b^*)$	(τ, η)	Data
$\mathcal{S}[1]$	2.9 (9)	3.0 (9)	(2.9, 1.3)	1.6915, 2.0847, 2.1003, 2.3745, 2.4215, 2.5860, 2.6215, 2.6805, 2.8680
	1.2 (9)	1.3 (9)		0.6015, 0.6897, 0.6973, 0.7165, 0.7855, 0.8545, 0.8895, 1.1157, 1.1313
$\mathcal{S}[2]$	2.5 (5)	2.7 (8)	(2.6805, 1.1157)	1.6915, 2.0847, 2.1003, 2.3745, 2.4215, 2.5860, 2.6215, 2.6805
	0.8 (5)	1.2 (8)		0.6015, 0.6897, 0.6973, 0.7165, 0.7855, 0.8545, 0.8895, 1.1157
$\mathcal{S}[3]$	2.5 (5)	2.6 (6)	(2.6, 0.9)	1.6915, 2.0847, 2.1003, 2.3745, 2.4215, 2.5860
	0.8 (5)	0.9 (6)		0.6015, 0.6897, 0.6973, 0.7165, 0.7855, 0.8545
$\mathcal{S}[4]$	1.7 (1)	2.1 (2)	(2.3745, 0.7165)	1.6915, 2.0847, 2.1003, 2.3745
	0.65 (2)	0.7 (3)		0.6015, 0.6897, 0.6973, 0.7165

Table 12: Estimates of $\mu_i,\ i = 1, 2,\ \beta$, and $\mathfrak{R}$ from WOLED datasets

Sample	Par.	MLE MPSE		MCMC LF-based MCMC SF-based		95% ACI-LF 95% ACI-SF			95% BCI-LF 95% BCI-SF		
		Est.	SE	Est.	SE	Low.	Upp.	IL	Low.	Upp.	IL
$\mathcal{S}[1]$	μ_1	1.5497	0.4022	1.5466	0.0104	0.7614	2.3380	1.5766	1.5267	1.5661	0.0394
		1.7138	0.4317	1.7128	0.0100	0.8677	2.5599	1.6921	1.6931	1.7323	0.0392
	μ_2	4.2814	1.2555	4.2800	0.0100	1.8207	6.7420	4.9214	4.2607	4.2994	0.0388
		3.4809	1.1504	3.4798	0.0101	1.2262	5.7356	4.5094	3.4602	3.4994	0.0392
	β	0.3700	0.1423	0.3587	0.0150	0.0910	0.6489	0.5579	0.3394	0.3782	0.0388
		0.1014	0.0417	0.0998	0.0095	0.0196	0.1832	0.1636	0.0819	0.1181	0.0362
	$\mathfrak{R}$	0.2658	0.0729	0.2654	0.0014	0.1229	0.4086	0.2857	0.2628	0.2680	0.0052
		0.3299	0.0812	0.3298	0.0014	0.1708	0.4891	0.3183	0.3270	0.3327	0.0056
$\mathcal{S}[2]$	μ_1	1.5020	0.4283	1.4992	0.0103	0.6626	2.3414	1.6788	1.4799	1.5189	0.0389

(Continued)

Table 12 (continued)

Sample	Par.	MLE MPSE		MCMC LF-based MCMC SF-based		95% ACI-LF 95% ACI-SF			95% BCI-LF 95% BCI-SF		
		Est.	SE	Est.	SE	Low.	Upp.	IL	Low.	Upp.	IL
		1.6372	0.4646	1.6363	0.0100	0.7266	2.5478	1.8212	1.6167	1.6560	0.0392
	μ_2	4.0753	1.3390	4.0741	0.0101	1.4508	6.6997	5.2489	4.0548	4.0942	0.0394
		3.7715	1.5342	3.7704	0.0101	0.7644	6.7785	6.0141	3.7507	3.7902	0.0394
	β	0.3607	0.1467	0.3528	0.0127	0.0732	0.6482	0.5749	0.3338	0.3721	0.0383
		0.1172	0.0506	0.1157	0.0097	0.0181	0.2164	0.1982	0.0971	0.1344	0.0373
	$\mathfrak{R}$	0.2693	0.0860	0.2690	0.0014	0.1008	0.4378	0.3369	0.2663	0.2717	0.0054
		0.3027	0.1024	0.3026	0.0014	0.1020	0.5034	0.4013	0.2999	0.3054	0.0055
$\mathcal{S}[3]$	μ_1	1.3516	0.4781	1.3496	0.0102	0.4146	2.2885	1.8739	1.3300	1.3692	0.0392
		1.4451	0.5422	1.4442	0.0101	0.3824	2.5079	2.1255	1.4246	1.4639	0.0393
	μ_2	3.5497	1.3784	3.5486	0.0101	0.8481	6.2512	5.4031	3.5293	3.5684	0.0391
		3.6217	1.5913	3.6206	0.0101	0.5029	6.7406	6.2377	3.6010	3.6404	0.0394
	β	0.3251	0.1526	0.3203	0.0111	0.0260	0.6242	0.5982	0.3013	0.3400	0.0387
		0.1354	0.0703	0.1339	0.0099	0.0009	0.2732	0.2723	0.1149	0.1531	0.0382
	$\mathfrak{R}$	0.2758	0.1120	0.2755	0.0016	0.0563	0.4952	0.4389	0.2724	0.2786	0.0062
		0.2852	0.1269	0.2851	0.0015	0.0364	0.5340	0.4976	0.2822	0.2881	0.0060
$\mathcal{S}[4]$	μ_1	1.3267	0.6045	1.3253	0.0101	0.1420	2.5114	2.3694	1.3058	1.3449	0.0391
		1.4218	0.7344	1.4209	0.0101	0.0000	2.8612	2.8612	1.4013	1.4406	0.0393
	μ_2	3.1055	1.4218	3.1044	0.0101	0.3189	5.8921	5.5732	3.0850	3.1242	0.0391
		3.3030	1.9838	3.3019	0.0101	0.0000	7.1913	7.1913	3.2823	3.3217	0.0394
	β	0.2445	0.1411	0.2415	0.0105	0.0032	0.5211	0.5179	0.2221	0.2612	0.0391
		0.1217	0.0832	0.1200	0.0100	0.0000	0.2848	0.2848	0.1009	0.1394	0.0385
	$\mathfrak{R}$	0.2993	0.1468	0.2992	0.0017	0.0116	0.5871	0.5756	0.2958	0.3025	0.0067
		0.3009	0.1846	0.3009	0.0016	0.0000	0.6626	0.6626	0.2977	0.3040	0.0064

For the Bayesian analyses we avoid extremely diffuse Gamma(0.001, 0.001)-type priors because they can be numerically unstable and place undue mass in extreme parameter regions. Instead, when no substantive expert input is available we adopt weakly-informative priors that ensure positive support while allowing the likelihood to dominate:

$$\beta \sim \text{Gamma}(2, 1), \qquad \mu \sim \text{Gamma}\big(2,\ \text{scale} = \hat{\mu}/2\big),$$

where $\hat{\mu}$ is a preliminary point estimate (we use the MLE). When an expert supplies a 50% quantile (median) m_0 for the lifetime, we translate it to a prior center for μ via $\mu_0 = m_0/(\ln 2)^{1/\beta^*}$, where β^* is either an expert guess for the shape or a pilot estimate; then μ can be given a Gamma prior with mean μ_0 and concentration chosen to reflect the expert's confidence.

To guard against prior-data conflict we perform prior predictive checks: for each prior $p(\beta, \mu)$ we draw (β, μ) from p, simulate n observations under Weibull (β, μ), compute the dataset median T, and compare the observed median T_{obs} to the prior predictive distribution of T. We report lower-tail, upper-tail and two-sided prior-predictive p-values; small two-sided p (near 0) indicates conflict.

Applied to the M00071 OLED sample (observed median $T_{\text{obs}} = 2503.75$), we obtain the following prior-predictive results (4000 prior predictive draws each):

– vague $Gamma(0.001, 0.001)$ priors: $p_{\text{low}} = 0.9463$, $p_{\text{up}} = 0.0537$, $p_2 = 0.1075$.

– weakly-informative priors: $\beta \sim \text{Gamma}(2, 1)$, $\mu \sim \text{Gamma}(2,\ \text{scale} = \hat{\mu}/2)$: $p_{\text{low}} = 0.6998$, $p_{\text{up}} = 0.3002$, $p_2 = 0.6005$.

– informative prior matching expert median $m_0 = 2500$: $p_2 = 0.9290$ (good agreement).

– conflicting informative prior with $m_0 = 1000$: $p_2 \approx 0$ (clear prior-data conflict).

When a prior-data conflict is detected (small two-sided p), we either (i) reconsider and possibly relax the prior concentration, (ii) revisit the elicited expert statement, or (iii) present sensitivity results (posterior under the informative prior vs. posterior under the weakly-informative default).

Due to the lack of informative prior knowledge on the Weibull model parameters from the WOLED studies, a joint improper gamma prior is employed in all Bayesian computations. The posterior summaries are generated using the proposed MCMC technique with a total of $\mathcal{M} = 50{,}000$ iterations, discarding the initial 10,000 iterations as burn-in. Starting values for the MCMC procedure are chosen based on the frequentist estimates of $\mu_i (i = 1, 2)$ and β, obtained via the ML and MPS methods (refer to Table 12). Results in Table 12 reveal that the Bayesian estimates, derived from the MCMC outputs, consistently achieve smaller SEs for $\mu_i (i = 1, 2)$, β, and $\mathfrak{R}$ compared to their frequentist analogs, indicating superior precision. Additionally, the BCIs against both LF-based and SF-based approaches tend to yield shorter ILs than their corresponding ACIs, thereby demonstrating greater efficiency in interval estimation.

To assess the existence and uniqueness properties of the MLEs and MPSEs for the parameters $\mu_i,\ i = 1, 2$, and β, Figs. 5 and 6 display the contour plots of the log-likelihood and log-spacing functions, respectively, evaluated based on the datasets $\mathcal{S}[i]$ for $i = 1, 2, 3, 4$. In Figs. 5 and 6, each contour plot illustrates a pair of parameters, with one on the horizontal axis and the other on the vertical axis, while the color bar represents the log-likelihood values. The red circle in the figure denotes the global maximum of the log-likelihood surface. The contours distinctly suggest that the WOLED data yield well-defined and unique solutions under both estimation frameworks. These graphical findings align with the numerical outcomes provided in Table 12. Additionally, to illustrate the posterior behavior, Fig. 7 focuses on sample $\mathcal{S}[1]$ and presents the Gaussian kernel density estimates along with trace plots for the parameters μ_1, μ_2, β, and $\mathfrak{R}$. Based on the remaining 40,000 MCMC draws of $\mu_i,\ i = 1, 2$, β, and $\mathfrak{R}$, the subplots in Fig. 7 demonstrate satisfactory mixing and stationarity, indicating a well-calibrated burn-in phase that effectively discards initial non-stationary iterations. Moreover, the posterior density estimates of μ_1, μ_2, β, and $\mathfrak{R}$ reveal that their marginal posterior distributions exhibit near-symmetrical shape, confirming the superiority and interpretability of the Bayesian inference. Furthermore, Table 13 presents a comprehensive summary of descriptive measures for the We parameters, encompassing the mean, mode, quartiles (denoted by Quart.i for $i = 1, 2, 3$), standard deviation (SD), and skewness (Skew.). These statistics confirm the same findings listed in Table 12.

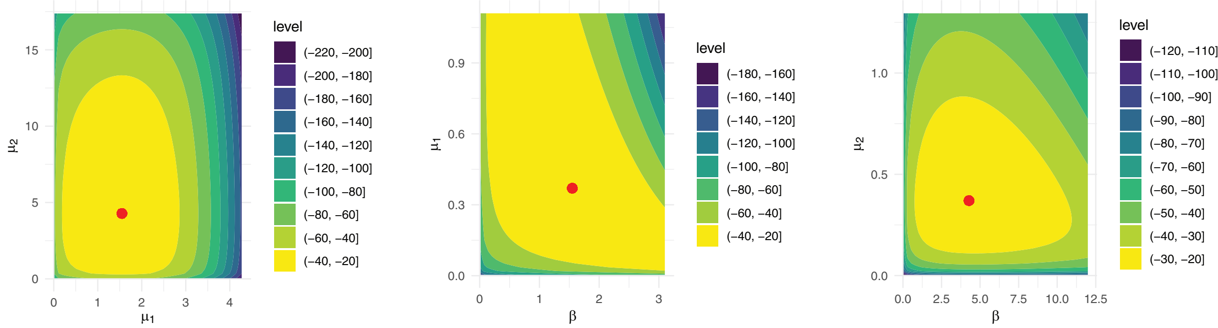

(a) Sample $\mathcal{S}[1]$

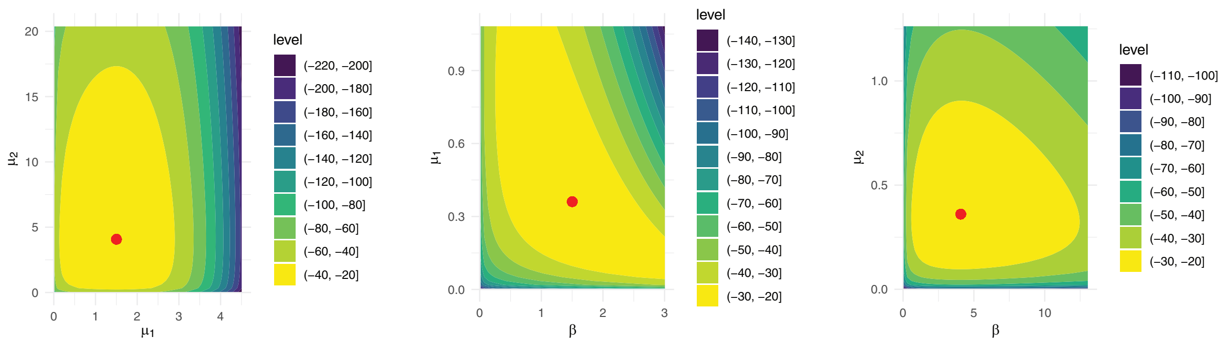

(b) Sample $\mathcal{S}[2]$

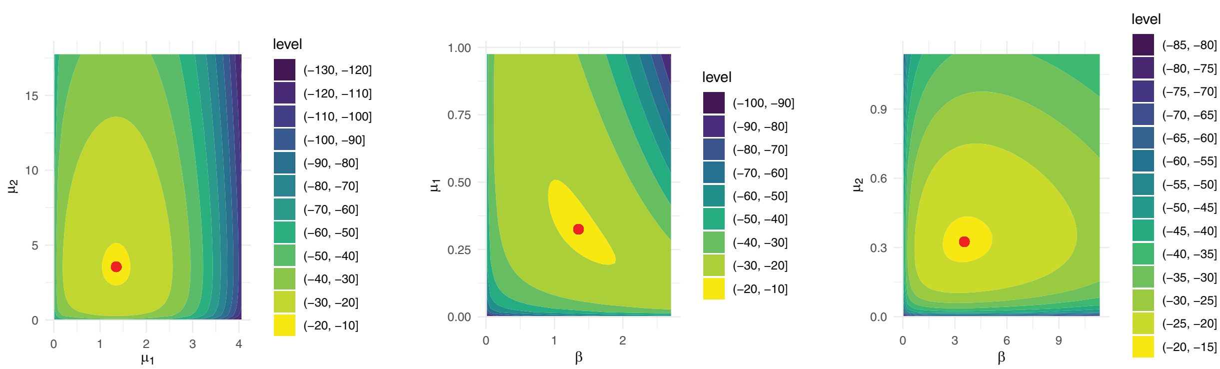

(c) Sample $\mathcal{S}[3]$

Figure 5: Contours from log-LF for $\mu_i,\ i = 1, 2,$ and β from WOLED datasets. (**a**): Sample $\mathcal{S}[1]$; (**b**): Sample $\mathcal{S}[2]$; (**c**): Sample $\mathcal{S}[3]$

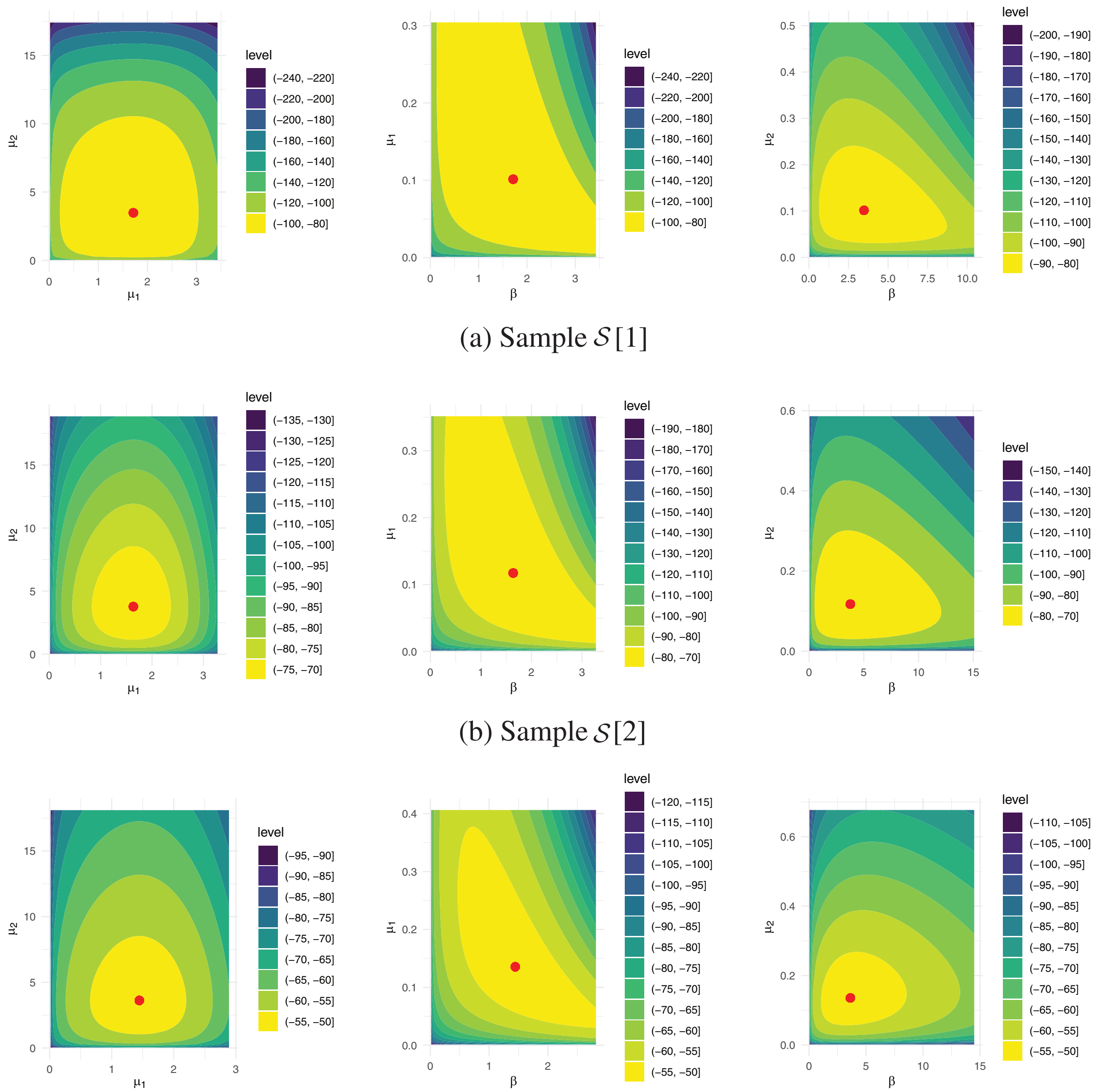

(a) Sample $\mathcal{S}[1]$

(b) Sample $\mathcal{S}[2]$

(c) Sample $\mathcal{S}[3]$

Figure 6: Contours from log-SF for $\mu_i,\ i = 1, 2$, and β from WOLED datasets. (**a**): Sample $\mathcal{S}[1]$; (**b**): Sample $\mathcal{S}[2]$; (**c**): Sample $\mathcal{S}[3]$

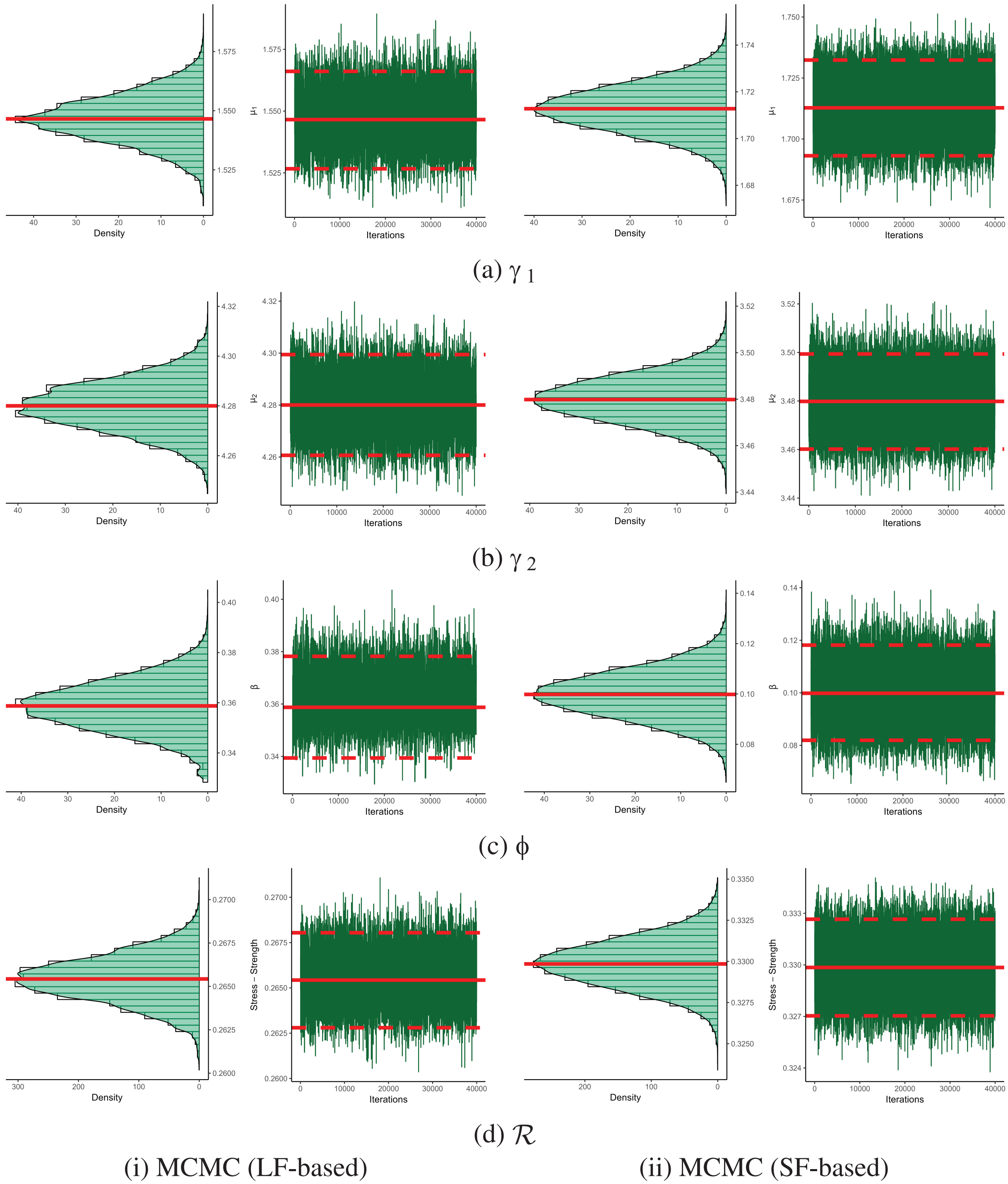

Figure 7: The MCMC diagrams of $\mu_i,\ i = 1, 2, \beta$, and $\mathfrak{R}$ from WOLED datasets. (**a**): γ_1; (**b**): γ_2; (**c**): ϕ; (**d**): $\mathcal{R}$

Table 13: Statistics of $\mu_i,\ i=1,2,\ \beta$, and $\mathfrak{R}$ from WOLED data

Sample	Par.	Mean	Mode	Quart.1	Quart.2	Quart.3	SD	Skew.
				MCMC (LF-based) MCMC (SF-based)				
$\mathcal{S}[1]$	μ_1	1.5466	1.5530	1.5401	1.5464	1.5531	0.0099	0.0138
		1.7128	1.7126	1.7061	1.7128	1.7195	0.0100	−0.0212
	μ_2	4.2800	4.2771	4.2733	4.2800	4.2869	0.0099	0.0066
		3.4798	3.4577	3.4731	3.4798	3.4867	0.0100	−0.0084
	β	0.3587	0.3317	0.3520	0.3587	0.3654	0.0099	0.0106
		0.0998	0.0891	0.0935	0.0998	0.1061	0.0093	0.0439
	$\mathfrak{R}$	0.2654	0.2664	0.2645	0.2654	0.2663	0.0013	−0.0057
		0.3298	0.3312	0.3289	0.3299	0.3308	0.0014	−0.0186
$\mathcal{S}[2]$	μ_1	1.4992	1.4821	1.4925	1.4990	1.5060	0.0100	0.0452
		1.6363	1.6294	1.6296	1.6363	1.6429	0.0100	0.0226
	μ_2	4.0741	4.0833	4.0672	4.0741	4.0809	0.0100	0.0453
		3.7704	3.7515	3.7637	3.7703	3.7771	0.0100	0.0114
	β	0.3528	0.3354	0.3461	0.3527	0.3593	0.0099	−0.0166
		0.1157	0.1083	0.1092	0.1156	0.1221	0.0095	0.0285
	$\mathfrak{R}$	0.2690	0.2663	0.2681	0.2690	0.2700	0.0014	−0.0081
		0.3026	0.3028	0.3017	0.3026	0.3036	0.0014	0.0138
$\mathcal{S}[3]$	μ_1	1.3496	1.3288	1.3428	1.3496	1.3565	0.0100	0.0215
		1.4442	1.4313	1.4375	1.4441	1.4508	0.0100	0.0236
	μ_2	3.5486	3.5426	3.5418	3.5486	3.5554	0.0100	0.0300
		3.6206	3.6170	3.6139	3.6206	3.6274	0.0100	0.0125
	β	0.3203	0.3079	0.3136	0.3202	0.3269	0.0100	−0.0108
		0.1339	0.1179	0.1273	0.1338	0.1404	0.0097	0.0306
	$\mathfrak{R}$	0.2755	0.2728	0.2745	0.2755	0.2766	0.0016	−0.0091
		0.2851	0.2835	0.2841	0.2851	0.2861	0.0015	0.0155
$\mathcal{S}[4]$	μ_1	1.3253	1.3044	1.3185	1.3253	1.3321	0.0100	0.0157
		1.4209	1.4080	1.4142	1.4208	1.4275	0.0100	0.0238
	μ_2	3.1044	3.1018	3.0976	3.1044	3.1112	0.0100	0.0212
		3.3019	3.2983	3.2952	3.3019	3.3087	0.0100	0.0153
	β	0.2415	0.2082	0.2348	0.2415	0.2482	0.0100	−0.0248
		0.1200	0.1042	0.1134	0.1200	0.1266	0.0098	0.0274
	$\mathfrak{R}$	0.2992	0.2957	0.2980	0.2992	0.3003	0.0017	−0.0164
		0.3009	0.2992	0.2998	0.3009	0.3019	0.0016	0.0148

Briefly, to account for external stressors (e.g., temperature, current density) we extend the Weibull model so that the scale parameter depends on covariates. Let z_i denote the covariate vector for unit i and set

$$\mu_i = \mu_0 \exp(\gamma^\top z_i),$$

so that the density of observation t_i is

$$f(t_i \mid \beta, \mu_0, \gamma) = \frac{\beta}{\mu_i}\left(\frac{t_i}{\mu_i}\right)^{\beta-1} \exp\left\{-\left(\frac{t_i}{\mu_i}\right)^{\beta}\right\}.$$

The log-likelihood is $\ell(\beta, \mu_0, \gamma) = \sum_{i=1}^{n}\left[\log\beta - \beta\log\mu_i + (\beta-1)\log t_i - (t_i/\mu_i)^\beta\right]$. Estimation can proceed by MLE (numerical optimization) or within our Bayesian framework by placing priors on $\log\beta, \log\mu_0$ and γ. In the LED M00071 example we illustrate the effect of including a two-level stress indicator (binary z) as a demonstration: the covariate model yields $\hat{\gamma} = 0.1954$ (SE 0.0437), and reduces the standard error of group median estimates compared with a pooled model (pooled SE of the median ≈ 107.8 vs. group SEs ≈ 77.0 and ≈ 86.9). The AIC improves by ≈ 8.4 when the covariate is included. These results are illustrative; for industrial inference we recommend recording physical stress covariates and fitting the extended model above so that one can quantify the effect of stress on lifetime and achieve the precision gains demonstrated here.

The analysis of WOLED devices under varying stress and strength conditions reveals key insights into their degradation patterns, enhancing predictive accuracy within life testing frameworks. Comparative evaluation across two WOLED datasets confirms the efficacy of the proposed statistical inference methods in modeling lifetime distributions using the We lifespan model under the recommended censoring scheme.

7 Concluding Remarks

This study comprehensively investigated classical and Bayesian estimation methodologies for the stress-strength reliability parameter under a unified hybrid censoring scheme, where X and Y follow independent Weibull distributions with a common shape parameter and different scale parameters. Four estimation approaches, namely, maximum likelihood estimation, maximum product of spacings, and Bayesian frameworks based on likelihood and spacing functions, were investigated, marking the first integration of the maximum product of spacings method within the unified hybrid censoring methodology. Bayesian estimates were derived under the squared error loss function, assuming independent gamma prior distributions for the three parameters. Samples from the posterior distribution derived based on the likelihood function were generated using the Metropolis-Hastings algorithm within the Gibbs sampling procedure. In contrast, the Metropolis-Hastings algorithm alone was employed to generate samples from the posterior distribution derived from the spacing function. To compare the various point and interval estimators, an extensive simulation study was conducted to evaluate their numerical accuracy and efficiency. Finally, illustrative application using light-emitting diode datasets were provided to demonstrate the practical utility of the proposed methods. Although the assumption of a common shape parameter is adopted in this study to simplify estimation, future research could relax this constraint to examine the robustness of classical and Bayesian methods when the stress and strength Weibull distributions have distinct shape parameters. Such extensions would broaden the applicability of the methods to a wider range of reliability scenarios.

Acknowledgement: Not applicable.

Funding Statement: This research was funded by Princess Nourah bint Abdulrahman University Researchers Supporting Project number (PNURSP2025R50), Princess Nourah bint Abdulrahman University, Riyadh, Saudi Arabia.

Author Contributions: The authors confirm contribution to the paper as follows: study conception and design: Mazen Nassar, Refah Alotaibi; data collection: Ahmed Elshahhat; analysis and interpretation of results: Mazen Nassar, Refah Alotaibi, Ahmed Elshahhat; draft manuscript preparation: Mazen Nassar, Refah Alotaibi, Ahmed Elshahhat. All authors reviewed the results and approved the final version of the manuscript.

Availability of Data and Materials: Data available within the article.

Ethics Approval: Not applicable.

Conflicts of Interest: The authors declare no conflicts of interest to report regarding the present study.

References

1. Birnbaum ZW, McCarty RC. A distribution-free upper confidence bound for $P(Y< X)$, based on independent samples of X and Y. Annals Math Stat. 1958;29(2):558–62.
2. Kotz S, Lumelskii Y, Pensky M. The stress-strength model and its generalizations: theory and applications. New York, NY, USA: World Scientific; 2003.
3. Asgharzadeh A, Valiollahi R, Raqab MZ. Stress-strength reliability of Weibull distribution based on progressively censored samples. SORT-Statis Oper Res Trans. 2011;35(2):103–24. doi:10.1016/j.csda.2010.02.005.
4. Kundu D, Gupta RD. Estimation of $P[Y < X]$ for Weibull distributions. IEEE Trans Reliab. 2006;55(2):270–80.
5. Pundir PS, Gupta PK. Stress-strength reliability of two-parameter bathtub-shaped lifetime model based on hybrid censored samples. J Stat Manage Syst. 2018;21(7):1229–50. doi:10.1080/09720510.2018.1496521.
6. Jana N, Kumar S, Chatterjee K. Inference on stress-strength reliability for exponential distributions with a common scale parameter. J Appl Stat. 2019;46(16):3008–31. doi:10.1080/02664763.2019.1625878.
7. Kumari R, Tripathi YM, Wang L, Sinha RK. Reliability estimation for Kumaraswamy distribution under block progressive type-II censoring. Statistics. 2024;58(1):142–75. doi:10.1080/02331888.2024.2301736.
8. Kotb MS, Al Omari MA. Estimation of the stress-strength reliability for the exponential-Rayleigh distribution. Math Comput Simul. 2025;228:263–73. doi:10.1016/j.matcom.2024.09.005.
9. Lai CD, Murthy DN, Xie M. Weibull distributions and their applications. In: Springer handbooks. London, UK: Springer; 2006. p. 63–78. doi:10.1007/978-1-84628-288-1_3.
10. Cavalcante T, Ospina R, Leiva V, Cabezas X, Martin-Barreiro C. Weibull regression and machine learning survival models: methodology, comparison, and application to biomedical data related to cardiac surgery. Biology. 2023;12(3):442. doi:10.3390/biology12030442.
11. Almarashi AM, Algarni A, Nassar M. On estimation procedures of stress-strength reliability for Weibull distribution with application. PLoS One. 2020;15(8):e0237997. doi:10.1371/journal.pone.0237997.
12. Balakrishnan N, Kundu D. Hybrid censoring: models, inferential results and applications. Comput Statis Data Anal. 2013;57(1):166–209.

13. Chandrasekar B, Childs A, Balakrishnan N. Exact likelihood inference for the exponential distribution under generalized Type-I and Type-II hybrid censoring. Naval Res Logist. 2004;51:994–1004. doi:10.1002/nav.20038.
14. Balakrishnan N, Rasouli A, Sanjari Farsipour N. Exact likelihood inference based on an unified hybrid censored sample from the exponential distribution. J Stat Comput Simul. 2008;78(5):475–88. doi:10.1080/00949650601158336.
15. Hasaballah MM, Tashkandy YA, Balogun OS, Bakr ME. Statistical inference of unified hybrid censoring scheme for generalized inverted exponential distribution with application to COVID-19 data. AIP Adv. 2024;14(4):045111. doi:10.1063/5.0201467.
16. Kumar K, Kumar S, Garg R, Kumar I. Reliability estimation for inverse Pareto lifetime model based on unified hybrid censored data. Int J Syst Assur Eng Manage. 2024;15(6):2473–82. doi:10.1007/s13198-024-02265-3.
17. Hasaballah MM, Balogun OS, Bakr ME. Bayesian estimation for the power rayleigh lifetime model with application under a unified hybrid censoring scheme. Phys Scr. 2024;99(10):105209. doi:10.1088/1402-4896/ad72b2.
18. Shukla AK, Soni S, Kumar K. Statistical inference and prediction in unified hybrid censored power Lindley distribution. Life Cycle Reliability Saf Eng. 2025;14:183–204. doi:10.1007/s41872-024-00295-1.
19. Cheng RCH, Amin NAK. Estimating parameters in continuous univariate distributions with a shifted origin. J R Statis Soc: Series B (Methodol). 1983;45(3):394–403. doi:10.1111/j.2517-6161.1983.tb01268.x.
20. Ranneby B. The maximum spacing method. An estimation method related to the maximum likelihood method. Scand J Stat. 1984;11(2):93–112.
21. Anatolyev S, Kosenok G. An alternative to maximum likelihood based on spacings. Econom Theory. 2005;21(2):472–6. doi:10.1017/s0266466605050255.
22. Hu X, Ren H. Statistical inference of the stress-strength reliability for inverse Weibull distribution under an adaptive progressive type-II censored sample. AIMS Math. 2023;8(12):28465–87. doi:10.3934/math.20231457.
23. Kotb MS, Raqab MZ. Inferential analysis of the stress-strength reliability for a new extended family of distributions. Res Stat. 2025;3(1):2452926. doi:10.1080/27684520.2025.2452926.
24. Kateri M, Nikolov NI. Product of spacings estimation in step-stress accelerated life testing: an alternative to maximum likelihood. IEEE Trans Reliab. 2024;73(3):1433–45. doi:10.1109/tr.2024.3369977.
25. Sayyareh A, Panahi H. Model selection based on tracking interval under unified hybrid censored. Samples J Iran Stat Soc. 2022;17(1):1–31. doi:10.29252/jirss.17.1.1.
26. Wang QA, Wang HB, Ma ZG, Ni YQ, Liu ZJ, Jiang J, et al. Towards high-accuracy data modelling, uncertainty quantification and correlation analysis for SHM measurements during typhoon events using an improved most likely heteroscedastic Gaussian process. Smart Struct Syst. 2023;32(4):267–79.
27. Wang QA, Liu Q, Ma ZG, Wang JF, Ni YQ, Ren WX, et al. Data interpretation and forecasting of SHM heteroscedastic measurements under typhoon conditions enabled by an enhanced Hierarchical Sparse Bayesian Learning model with high robustness. Measurement. 2024;230:114509. doi:10.1016/j.measurement.2024.114509.
28. Dey S, Elshahhat A, Nassar M. Analysis of progressive type-II censored gamma distribution. Comput Stat. 2023;38(1):481–508. doi:10.1007/s00180-022-01239-y.
29. Kurdi T, Nassar M, Alam FMA. Bayesian estimation using product of spacing for modified kies exponential progressively censored data. Axioms. 2023;12(10):917. doi:10.3390/axioms12100917.
30. Nassar M, Elshahhat A. Estimation procedures and optimal censoring schemes for an improved adaptive progressively type-II censored Weibull distribution. J Appl Stat. 2024;51(9):1664–88. doi:10.1080/02664763.2023.2230536.

31. Henningsen A, Toomet O. maxLik: a package for maximum likelihood estimation in R. Comput Stat. 2011;26:443–58. doi:10.1007/s00180-010-0217-1.
32. Plummer M, Best N, Cowles K, Vines K. CODA: convergence diagnosis and output analysis for MCMC. R News. 2006;6:7–11.
33. Farinola GM, Ragni R. Electroluminescent materials for white organic light emitting diodes. Chem Soc Rev. 2011;40(7):3467–82. doi:10.1039/c0cs00204f.
34. Zhang J, Cheng G, Chen X, Han Y, Zhou T, Qiu Y. Accelerated life test of white OLED based on lognormal distribution. Indian J Pure Appl Phys (IJPAP). 2015;52(10):671–7.